

Neural and Behavioral Correlates of Saccadic Eye Movements to Moving Targets

by

Kevin John Mohsenian

Bachelor in Biomedical Engineering, University of Minnesota -Twin Cities, 2012

Master of Science in Biomedical Engineering, University of Minnesota -Twin Cities, 2014

Submitted to the Graduate Faculty of the
Swanson School of Engineering in partial fulfillment
of the requirements for the degree of
Doctor of Philosophy

University of Pittsburgh

2021

UNIVERSITY OF PITTSBURGH

SWANSON SCHOOL OF ENGINEERING

This dissertation was presented

by

Kevin John Mohsenian

It was defended on

March 25, 2021

and approved by

Dr. Aaron Batista, PhD, Professor, Bioengineering

Dr. Carol Colby, PhD, Professor, Neuroscience

Dr. Matthew Smith, PhD, Associate Professor, Biomedical Engineering (CMU)

Dissertation Director: Dr. Neeraj Gandhi, PhD, Professor, Bioengineering

Copyright © by Kevin John Mohsenian

2021

Neural and Behavioral Correlates of Saccadic Eye Movements to Moving Targets

Kevin John Mohsenian, PhD

University of Pittsburgh, 2021

The ability to catch moving objects with our line of sight is crucial for survival in our dynamic everyday environment, such as determining if the insect buzzing toward your head is a harmless fly or a “killer hornet.” Saccades, or rapid eye movements, are employed to shift our gaze to intercept moving targets. Due to an inherent neural transduction delay (~100ms), the *sensory representation* of a moving target’s position lags the target’s *actual position*. Fortunately, this discrepancy in target encoding does not hinder humans and non-human primates from intercepting moving targets, as both species can accurately catch a moving stimulus with their gaze. The oculomotor system could overcome this transmission delay by integrating the *velocity* of the target over the delay and adding it to the neural representation of the target’s *position*. How position and velocity information are combined to program saccades to moving targets (interceptive saccades) is currently unknown.

In this study, we investigated the behavior and neural correlates of interceptive saccades. We found a consistent decrease in peak velocity for interceptive saccades compared to amplitude-matched saccades to static targets (control). The greatest reduction in peak velocity occurred between target speeds of 10-40 deg/s. We also investigated the superior colliculus (SC) as a possible location to combine position and velocity information, as it is the sensorimotor integration hub for the oculomotor system. We discovered that the SC population activity changes from a symmetrically-distributed activity to a streaked mound of activity for interceptive saccades, and

the streak spreads along the target's trajectory. The spread of the streak was also dependent on the speed of the moving stimulus. Our data are consistent with the interpretation that the SC reflects both the moving target's position and velocity. Many neurological disorders, such as Parkinson's and Alzheimer's disease, cause a decrease in the ability to make predictive movements. We anticipate that once the interceptive saccade mechanism is determined, interceptive saccades can be used as non-invasive biomarkers to monitor patient health and track disease progression.

Table of Contents

Acknowledgements	xi
1.0 Introduction – General Background on the Importance of Eye Movements	1
1.1 The Behavioral Metrics of Saccades	3
1.1.1 The Behavior of Saccades to Static Targets.....	3
1.1.2 The Behavior of Saccades to Moving Targets	5
1.2 Neural Correlates of Saccades to Static Targets	7
1.2.1 Superior Colliculus Activity for Stationary Saccades.....	9
1.3 Neural Correlates for Saccades to Moving Targets	12
1.3.1 Superior Colliculus Activity for Interceptive Saccades.....	14
1.4 Knowledge Gaps and Research Strategies	14
2.0 Behavioral Metrics of Interceptive Saccades in the Rhesus Macaque.....	17
2.1 Introduction	17
2.2 Methods	18
2.3 Results.....	26
2.4 Discussion	38
3.0 Superior colliculus population activity analysis for interceptive saccades.....	48
3.1 Introduction	48
3.2 Methods	51
3.3 Results.....	57
3.4 Discussion	68
4.0 Neural Network Model of the Superior Colliculus	76

4.1 Methods	76
4.2 Results.....	79
4.3 Discussion	80
5.0 Conclusions and Future Directions	83
5.1 Conclusions	83
5.2 Future Directions.....	84
Bibliography	90

List of Tables

Table 1: Number of Movements Collected for Each Trial Type 27

Table 2: Comparison for Vector Averaging and Vector Summation Estimations 67

**Table 3: Maximum Eye Velocity and Firing Rate Attained During Stationary and Moving
Conditions 68**

List of Figures

Figure 1: Delay Saccade Task for an Outward Moving Target	20
Figure 2: Amplitude-Matched Saccade Profiles for Static and Moving Targets	21
Figure 3: Session Combining Method	22
Figure 4: Main Sequence Comparison Between Moving and Stationary Trials	28
Figure 5: The Attenuation of Peak Velocity for Interceptive Saccades	30
Figure 6: Saccade Duration Comparison Between Moving and Stationary Trials	32
Figure 7: Saccade Latency Comparison Between Moving and Stationary Trials	33
Figure 8: Saccade Error Comparison Between Moving and Stationary Trials.....	34
Figure 9: Saccadic Error as a Function of Target Speed	36
Figure 10: Average Pursuit Gain for Interceptive Movements	38
Figure 11: Peak Velocity Attenuation Pattern Across Subjects	42
Figure 12: Dual Drive vs. Streaked Activity Hypotheses	50
Figure 13: Experimental Setup.....	58
Figure 14: Data Alignment for SC Recordings	59
Figure 15: Estimating the Preferred Vector Encoded by the Recorded Neuron	61
Figure 16: Neuron Distribution and Transformation	62
Figure 17: Average SC Population Activity for Different Movement Sizes	63
Figure 18: Population Activity in the SC for Stationary and Outward Moving Targets.....	64
Figure 19: Population Activity in the SC for Stationary and Inward Moving Targets	65
Figure 20: The Timecourse for Saccade Vector Estimation	67

Figure 21: Proposed Oculomotor Circuitry that Plans and Executes the Interceptive Saccade..... 72

Figure 22: The Model Transformation of the SC 76

Figure 23: Schematic of the Modified 1D Arai SC Model 77

Figure 24: Intralaminar Weights of SC Layers 79

Figure 25: Stationary and Moving Target Simulations of 1D SC model..... 80

Acknowledgements

I want to take a moment to share my gratitude for the people that were important and helped me along the way to completing my dissertation. First, I'd like to thank the most important people in my life – my family. My parents, Farhad and Cynthia, raised me to be independent thinking, and their expertise (Dad – structural engineering, Mom – medtech) shaped how I learned. My mom is someone who seems to know enough medical information to be a doctor herself, and after five kids, she has seen it all. She is one of my biggest supporters; she is always giving me the confidence to keep going. And my dad, who is someone I have always looked up to, helped to instill a love for math and equations. He has also been a constant source for guidance and professional advice. I decided early in high school that I wanted to do something that combined my parent's backgrounds of both science and math, and ended up finding the major of biomedical engineering. I am very grateful for my parents' love and support, and for their emphasis to instill a mindset to always stay curious and keep learning. I dedicate this work to my mother and father.

I have four siblings, Sarah, Melissa, Brian, and Leila, who have been a constant source of love and support. And without them I would not be the person I am today. They have motivated me, supported me, and given me the courage to push boundaries to always strive for more. I love them all so much.

The COVID-19 pandemic started about a year before I defended my dissertation, and working from home exclusively became very difficult. I would like to acknowledge the people that helped make this work possible given the pandemic barriers. Clara (postdoc in my lab), who has become a wonderful friend, helped to support me on a daily basis in the lab to complete my last months of experiments. Clara also joined me for writing sessions and zoom sessions to get

work done. Her positivity and diligence are attributes I will take with me going forward, and I will miss working with her. I also spent many hours on Zoom with my friend Erica, my labmate Michelle, and my sister Leila. All people who were also working on projects or writing papers while I worked on the dissertation. The important thing to keep in mind in life is to find what works for you, and I am very thankful that I have such a great supporting cast to be able to depend on. I am forever grateful.

I want to specifically thank my wife, Elizabeth, for her unconditional love and support over the course of my PhD program. Without her, I would not have been able to complete this work. She helped take care of everything else so that I could focus on my dissertation. I appreciate her and love her forever.

I would like to thank my graduate advisor, Dr. Neeraj (Raj) Gandhi, for his help in developing me into a strong leader and better scientist. His continued support of my ideas for new projects or analyses was appreciated and resulted in the quality work shown in this dissertation. It was an incredible experience to learn from Raj's expertise on saccades and the superior colliculus, and the main reason I have become an expert on saccades to moving targets. Every great scientist has a great mentor, and I am no exception to that rule.

I would also like to extend my gratitude to my dissertation committee: Dr. Aaron Batista, Dr. Carol Colby, and Dr. Matthew Smith. The committee met with me every other month for the year leading up to my defense, and they were a constant source of positivity and encouragement. Their support really helped me reach the finish line for the dissertation. I am very thankful for their time and continued support.

1.0 Introduction – General Background on the Importance of Eye Movements

The ability to catch moving objects with our line of sight is crucial for survival in our dynamic everyday environment, such as locating a deer on the road while driving and determining if it's going towards or away from the car's current driving lane. Saccades, or rapid eye movements, are implemented to shift our gaze to intercept moving targets. Due to an inherent neural transduction delay (50-100ms), the *sensory representation* of a moving target's position lags the target's *actual position* when the saccade is programmed to catch the moving object (Becker & Jürgens, 1979; Fleuriet, Hugues, Perrinet, & Goffart, 2011; Schlag & Schlag-Rey, 2002). Fortunately, this discrepancy between the target's neural representation and its actual location does not hinder humans and non-human primates from intercepting the moving target, as both can accurately catch moving targets (S. de Brouwer, Missal, Barnes, & Lefèvre, 2002; Eggert, Guan, Bayer, & Büttner, 2005; E Keller & Johnsen, 1990). One mechanism to overcome this transmission delay would be to integrate the *velocity* of the target over the transmission and add this to the neural representation of the target's *position* (Guan, Eggert, Bayer, & Büttner, 2005; EL Keller, Gandhi, & Weir, 1996; Robinson, 1973). How position and velocity are combined to make saccades to moving targets (interceptive saccades) is currently unknown.

The goal of this research project is to understand the behavioral and neural correlates of saccades that intercept moving targets, with the primary focus on characterizing population activity in the superior colliculus (SC). The minimum time interval to incorporate additional information about a moving target is approximately 50-100 milliseconds prior to an interceptive saccade onset due to an afferent transmission delay (Becker & Jürgens, 1979; Fleuriet et al., 2011). When a target

moves, a predictive movement is required to catch the moving stimulus, which would involve combining the last sampled position of the target with the distance the target travels during the transmission delay (EL Keller et al., 1996). It is unclear how the oculomotor system integrates the moving targets' velocity information to drive saccades to catch moving targets accurately. We aim to determine the difference in the behavioral characteristics and the SC population activity in saccades to moving targets.

Broader impacts of this work extend to changes in interceptive saccade metric changes being tracked and used as a biomarker for determining changes in neurophysiological pathologies that are sometimes difficult to track – schizophrenia, attention deficit disorder (Munoz, Armstrong, Hampton, & Moore, 2003; Reuter & Kathmann, 2004) – or in the disorders where titration of medication can be challenging to maintain – Parkinson's and Alzheimer's disease (Fletcher & Sharpe, 1986; White, Saint-Cyr, Tomlinson, & Sharpe, 1983). Interceptive saccades involve building an internal model of the moving stimulus to shift gaze onto them properly, and in these disorders, that process seems to be impaired (Braff & Geyer, 1990; Chan, Armstrong, Pari, Riopelle, & Munoz, 2005; TJ Crawford, Bennett, Lekwuwa, Shaunak, & Deakin, 2002; T. Crawford, Goodrich, Henderson, & Kennard, 1989; Fletcher & Sharpe, 1986; Kennard & Lueck, 1989; Munoz et al., 2003; Reuter & Kathmann, 2004; Terao et al., 2011; White et al., 1983). The more scientists can learn about interceptive saccade behavior, and the neural correlates that underlie them, the higher the potential is to create more tools for patients with these types of neurophysiological disorders.

1.1 The Behavioral Metrics of Saccades

Saccades, or rapid gaze shifts, are one of the fastest movements our bodies can make. Saccades are essential, as they redirect the fovea, the most sensitive part of the retina, onto objects of interest. The term saccade was first used to describe these fast eye movements in the 1800s (Javal, 1878; Landolt, 1891) and originates from the French language, referring to the jerk of a horse's head with a pull of the reins (Leigh & Zee, 2015).

1.1.1 The Behavior of Saccades to Static Targets

The saccade planning process is composed of two main components: a pulse and a step (Robinson 1968). The pulse is to initiate the movement and drive the maximum velocity attained during the saccadic eye movement, and the step is to determine the duration of the saccade to reach a specified movement size. A unique feature of saccades is that they are very stereotyped, specifically in terms of the predictability of peak velocity and duration given a specific movement size (amplitude). Previous reports of this relationship were first coined the “main sequence” of the saccades by Bahill et al., since the relationship was analogous to the relationship between the brightness and temperature of stars (Bahill, Clark, & Stark, 1975). The following non-linear equation can describe peak velocity:

$$PV = V_{max}(1 - e^{-\left(\frac{amp}{c}\right)}) \quad (1.1)$$

PV – peak velocity, Vmax – terminal velocity of the eye, amp – amplitude, C-constant fit to the individual

Similar to peak velocity, the duration of saccades is very stereotyped and predictable given a saccadic amplitude. In contrast to the non-linear relationship with peak velocity, the duration is linear as a function of saccade amplitude for eye movements in the range of 1° - 50° (Leigh & Zee, 2015).

The initiation time for a saccade, or latency, is often studied for saccades because it helps to understand the time needed for planning and generating a saccadic eye movement. The typical latency for a saccade is approximately 200 msec. Several factors about the experimental set-up can affect latency: target luminance, contrast, target size, and predictability of a target. These factors can allow scientists to investigate certain task types' effects on cognitive aspects, such as attention and motivation (Groner & Groner, 1989). For example, a memory-guided task is a trial where a peripheral target is flashed briefly on the screen while the subject is fixating on a central target. After some time, the central target is extinguished, and the subject makes a saccade to the flashed target location. In addition to these movements being slower and more prolonged (peak velocity and duration), the latency of these movements is longer than visually-guided trials when the peripheral target is maintained, rather than flashed, before and after the saccade. This increase in latency can be due to more uncertainty about the remembered location of the target.

Saccade inaccuracy or dysmetria can occur when the main components of the saccade planning (pulse and step) are not adequately coordinated. Typically subjects show small but measurable pulse dysmetria, undershooting (hypometria) about 10% for randomly-presented targets. Moreover, subjects will do a corrective saccade to bring the fovea closer to the desired target, approximately 150 msec after the initial saccade (Leigh & Zee, 2015).

1.1.2 The Behavior of Saccades to Moving Targets

While there is a strong understanding of saccades' behavior to stationary targets, or stationary saccades, the same cannot be stated for the understanding of the behavior for interceptive saccades or saccades to moving targets. Most studies for interceptive saccades typically compare the interceptive saccade metric with the same subject's stationary saccade metrics to essentially treating the stationary saccade metrics as a control (Fleuriet et al., 2011; EL Keller et al., 1996). The initial studies of saccades to moving targets originated from saccades made during smooth pursuit. Smooth pursuit is a slow eye movement used to track a target, keeping the gaze fixated on the moving stimulus (E. L. Keller & Heinen, 1991; Rashbass, 1961). If the distance between the gaze position and the moving stimulus becomes too large during the pursuit, the oculomotor system will generate a saccade, which we will refer to as a catch-up saccade, to bring the gaze position back onto the moving stimulus to allow for continued pursuit. Understanding the programming of catch-up saccades can be difficult because the initial pursuit before the catch-up saccade can affect the initialization of the catch-up saccade, and the distance for catch-up saccades is typically small, so understanding the "main sequence" of catch-up saccades (S. de Brouwer et al., 2002). Therefore, the investigations included in this dissertation focused on interceptive saccades, which require an initial fixation prior to generating the saccade to catch a moving target. When considering interceptive saccade behavior, it is essential to consider three main components: target speed, target direction, and target trajectory. The behavioral study focused on four main metrics: peak velocity, duration, latency, and saccadic error.

Similar to stationary saccades, given previous reports, the expectation for interceptive saccade peak velocity and duration would be to follow the “main sequence” relationships, where a saturating exponential function best fits peak velocity as a function of saccade amplitude. In contrast, duration as a function of saccade amplitude is linear (Bahill et al., 1975). The critical difference between stationary and interceptive saccades would be the parameters to fit these functions, specifically if interceptive saccades were slower or faster for peak velocity and longer or shorter, respectively, in duration. The frustrating aspect, and most challenging component to interceptive saccade research, is the lack of consistency regarding the moving target parameters. Each study seems to have a different target speed range, movement range, or target trajectories, making it difficult to compare. A few studies have shown that interceptive saccades programmed to intercept outward (centrifugal) moving targets have a lower peak velocity than amplitude-matched stationary saccades (Eggert et al., 2005; Guan et al., 2005; EL Keller et al., 1996). Also, studies have shown that interceptive saccades to inward (centripetal) moving targets have a higher peak velocity for inward moving targets (Eggert et al., 2005; Guan et al., 2005).

A few studies found no difference in peak velocity as a function of speed nor as a function of saccade amplitude (Fleuriet et al., 2011) or as a function of target direction (Goffart, Cecala, & Gandhi, 2017). The problem with all these studies is that almost none of them have overlapping target speeds, and target trajectories, and target directions, so it is difficult to have a conclusive statement about interceptive saccade “main sequence” dynamics and kinematics.

An important interceptive saccade metric to study is latency, the reaction time for the subject to initiate a saccade. This period is particularly interesting for moving targets compared to the stationary target trials due to the extra components the moving target includes, such as target velocity and trajectory. The longer it takes to program and initiate the interceptive saccade

for outward moving targets, the further the target gets from the subject's current gaze position, which potentially makes it more difficult with longer latencies. In contrast, for inward moving targets, the longer the latency, the smaller the distance between the target and the subject's current gaze position. Therefore, one could predict that outward could have shorter latencies and inward could have longer latencies. The only study that thoroughly investigates interceptive saccade latency reported increased latencies for moving target trials compared to stationary target trials, but their results were inconsistent across subjects (Fleuriet et al., 2011). The success of an interceptive saccade is determined by the fovea's accurate placement on the moving target. Observations of the accuracy are measured through saccadic error or the relative distance between the target position and the gaze position at the saccade end position. Several studies have observed that as target speed increased, so does saccadic error (Fleuriet et al., 2011; Quinet & Goffart, 2015), but very few studies tie this error with other interceptive saccade metrics.

1.2 Neural Correlates of Saccades to Static Targets

Humans and non-human primate oculomotor systems can be simplified to a primary circuit, "black box", where the input to the circuit is light – sensory information, and the output is movement commands – observed saccadic eye movement. Unfortunately for researchers, this sensorimotor transformation that occurs in this "black box" is a complicated process. The visual information enters the oculomotor system through the eyes' retinas and mainly by the fovea, the retina's most sensitive area (Leigh & Zee, 2015). The light is encoded through cones and rods and converted into a neurological signal using neurotransmitters and action potentials in the retinal ganglion cells (Leigh & Zee, 2015). The visual information is taken from the retina to the

visual cortex (V1), located in the brain's occipital lobe, by the optic nerve. About 10% of these projections also project to the superficial layers of the superior colliculus, located on the roof of the brainstem (May, 2006). Multiple visual cortices then process the visual information in the parietal and temporal lobes of the brain. Both the location and the visual details of objects are processed in these cortical areas and sent to the thalamus. The thalamus then sends information to the superior colliculus about what information is most relevant and generates the subsequent eye movements (Leigh & Zee, 2015). The superior colliculus is thought to be a central hub for sensorimotor transformation and converts the visual information into a movement command, the activity of these neurons being sufficient to initiate a saccade (Gandhi & Katnani, 2011). The thalamus also sends a signal to 'turn off' the omnipause neurons (OPNs) which allows the movement to initiate (Gandhi & Keller, 1999). The OPNs are thought to be the gating mechanism that allows SC activity to be delivered to output structures downstream in the saccade program pathway (Everling, Paré, Dorris, & Munoz, 1998; Gandhi & Keller, 1999). The motor command travels from the superior colliculus to the burst generators in the brain stem. The cerebellum also sends additional motor commands to the burst generators through the caudal fastigial nucleus. The movement command (the amplitude, angle, and dynamics of the movement) is then converted in the burst generators. The burst generators' output to the motor neurons is in a muscle command, which activates the proper eye muscles to move the subject's gaze to the new desired location. The environment is resampled through the retina, and the visual encoding process restarts. The critical regions of interest for us are brain areas that convert the sensory information to the motor information in the oculomotor system, the superior colliculus (SC), and the frontal eye fields (FEFs) (Hanes & Wurtz, 2001; Robert H. Wurtz, Sommer, Paré,

& Ferraina, 2001). The studies conducted in this dissertation will focus on the SC and its role in the oculomotor system to program interceptive saccades.

1.2.1 Superior Colliculus Activity for Stationary Saccades

The superior colliculus (SC) is a necessary structure for saccades and plays a crucial role in orienting an animal's attention by controlling gaze (Gandhi & Katnani, 2011; Sparks & Hu, 2006). Evidence suggests that the SC is the central hub in the sensorimotor integration for eye movements, as both visual and movement information is retinotopically mapped and encoded within the SC (Gandhi & Katnani, 2011; Huerta, 1984; Ottes, Van Gisbergen, & Eggermont, 1986). The SC has seven distinct layers, but their physiological properties can be categorized into two main layers: the superficial layers and intermediate layers (Huerta, 1984; May, 2006). The superficial layers (SCs) are populated with "visual" neurons, which will fire action potentials for a target shown in their respective visual field, encompassing a patch of the visual environment relative to the subject's center of gaze (Krauzlis, Liston, & Carello, 2004; McPeck & Keller, 2002). The SCs inputs include: the retina, primary visual cortex (V1), extrastriate visual cortices (V2 and V4), pretectum, and parabigeminal nucleus (Hall & Moschovakis, 2003; Huerta, 1984). The SCs has output projections to: the intermediate layers of the SC, the lateral geniculate nucleus, the pretectum, and the parabigeminal nucleus (May, 2006). The intermediate layers (SCi), which reside ventral to the SCs layers, contain mostly "motor" neurons (neurons that burst for a movement to a location in space), and "visuomotor" neurons (neurons that burst for both the presentation of visual stimuli as well as the movement to a location in space) (Gandhi & Katnani, 2011; May, 2006; Munoz & Wurtz, 1995a, 1995b; Sparks & Hartwich-Young, 1989; R. H. Wurtz & Goldberg, 1972). Visuomotor neurons will have a visual field (area of visual space, relative to

the center of gaze, that the neuron will respond) and a movement field (movements relative to the center of gaze that the neuron would be active and contribute to the movement generation). The layers of the SC_i receive inputs from the SC_s layers, lateral interparietal area (LIP), frontal eye fields (FEF), the inferotemporal cortex (IT), dorsolateral prefrontal cortex (dlPFC), and the substantia nigra pars reticulata (SNpr) (May, 2006; Robert H. Wurtz et al., 2001). The SC_i layers project to the saccadic burst generators (BGs) in the paramedian pontine reticular formation (PPRF) for horizontal saccades and the medial reticular formation (MRF) for vertical saccades (Gandhi & Katnani, 2011; Hall & Moschovakis, 2003; John K Harting, 1977; May, 2006).

A vital feature of the SC is that within each layer resides a retinotopically organized map. The SC map corresponds to the contralateral visual hemifield. It is organized by saccade amplitude, which increases logarithmically along the rostral to caudal axis, and saccade angle, which is organized more linearly along the medial-lateral axis (upper hemifield (+90°) on the medial side, and lower hemifield (-90°) on the lateral side) (Katnani & Gandhi, 2012; McHaffie & Stein, 1982; Robinson, 1972; Stanford, Freedman, & Sparks, 1996; Straschill & Rieger, 1973). This map exists in both the SC_s and SC_i layers. There have been studies to support that similar response field locations on the map exist along the SC's dorsal-ventral axis, essentially creating "columns" of similar activity. However, while this interlaminar columnar structure exists in the SC, interlaminar connections are more sparse and not very strong (J. K. Harting, Hall, Diamond, & Martin, 1973). Most of the connections are thought to be feedback connections rather than feedforward connections (Phongphanphane et al., 2011). Given inactivation experiments, the SC population activity is theorized to encode the saccade vector as a function of population activity in the SC's intermediate layers (Lee, Rohrer, & Sparks, 1988).

Studies have investigated the intralaminar activity, or activity within a layer, for both the SCs and SCi, to understand how SC population activity is generated. Interestingly, both layers have a local-excitatory-global-inhibitory (LEGI) network, where glutamatergic neurons drive excitation close to the input's focal point to the SC (Pettit, Helms, Lee, Augustine, & Hall, 1999; Phongphanphanee et al., 2014). However, these neurons collaterally activate GABA-ergic interneurons that inhibit the activity of neighboring neurons (Meredith & Ramoa, 1998; Munoz & Istvan, 1998; Phongphanphanee et al., 2014). This LEGI network is essential for driving the Gaussian-like mound of activity in the SC for stationary targets and is primarily responsible for balancing the visual and motor burst activity seen in certain task types, such as the delay saccade activity (Anderson, Keller, Gandhi, & Das, 1998; Goossens & van Opstal, 2012). In the SCi visuomotor neurons, the delay period activity, between the visual and motor burst, is shaped by the LEGI network dynamics.

The SC encodes the saccade vector as a population, but it remains definitively determined how the population activity sends the saccade vector information downstream. The inactivation experiment mentioned before suspected that changes to the saccade vector, based on where the muscimol inactivation occurred in the SC map, suggests that downstream structures decode the SC population activity through an averaging mechanism, and therefore the average activity of the population determines the saccade vector magnitude and direction (Hall & Moschovakis, 2003; Lee et al., 1988; Ottes et al., 1986). Others have postulated that the SC could encode the saccade vector through a summation mechanism (Goffart et al., 2017; Katnani & Gandhi, 2012). For stationary targets, the SC population activity is approximated to be a hill-shaped mound of activity centered on the SC map at the intended saccade vector location (Anderson et al., 1998; Goossens & van Opstal, 2012; Lee et al., 1988). If the population activity is approximately symmetrical on

the SC map, then both vector summation and vector averaging will give the same estimated saccade vector. Stimulation and inactivation experiments are potential options to drive irregularities in the network, and these manipulations to the population have been attempted (Katnani & Gandhi, 2012; Lee et al., 1988), but none have been consistent and therefore the encoding mechanism is still debated (Goffart et al., 2017). Therefore, if there were a natural way to produce a non-Gaussian distribution in the SC population, this would allow for proper testing between the summation and averaging mechanisms. We anticipate that interceptive saccade population activity may present a non-gaussian response in the SC neural population.

1.3 Neural Correlates for Saccades to Moving Targets

When generating an interceptive saccade or a saccade to a moving target, the areas that transform the sensory information to movement commands are mostly the same. The two key differences are: 1) the target velocity will be encoded in specific areas that are sensitive to moving stimuli, adding information (and noise) to areas they are connected with, and 2) the target position changes throughout the time that the saccade is being programmed (during the transduction delay) which will activate and drive neurons differently in the oculomotor pathway. There are two main hypotheses that have been proposed for how the brain might compensate for these delays: the dual drive hypothesis (EL Keller et al., 1996) and the remapping hypothesis (Goffart et al., 2017). The dual drive hypothesis assumes that the last sampled position of the moving target (~100msec before saccade onset) is encoded by the SC population activity, and the target displacement during the transduction delay is integrated by a different structure and added downstream in the burst generators (Gandhi & Katnani, 2011). The alternative remapping hypothesis proposes that the SC

population activity can incorporate the velocity-related activity by updating the moving target across the map. The target traverses the screen before the interceptive saccade, and this updating causes a streak in the SC population activity, which has been reported previously (Dash, Yan, Wang, & Crawford, 2015). The streaked population activity would no longer be symmetrical mound of activity, and the extent of the streak would reveal the speed, direction, and trajectory of the moving stimulus, informing the saccade programming downstream. The streak could come from outside input from brain regions that encode moving targets, or the streak could be an intrinsic intralaminar LEGI network dynamic (Goffart et al., 2017; Meredith & Ramoa, 1998; Phongphanphane et al., 2014). Either way, the SC would essentially encode the interceptive saccade vector with its population activity.

There is a large amount of research on visual information regarding moving targets for smooth pursuit (see review, Wurtz 2001 (E. L. Keller & Heinen, 1991; Lisberger, Morris, & Tychsen, 1987)). From these studies, researchers have discovered the middle temporal area (MT) and the medial superior temporal area (MST) as two critical areas in the extrastriate cortex that are tuned to moving target velocity (speed and direction) and even have response fields (Wall, Symonds, & Kaas, 1982). MT and MST have outputs to many brain regions, but most notably, they project to the SC (mostly SCs), FEF, and the nucleus reticularis tegmenti pontine (NRTP) (Ungerleider, Desimone, Galkin, & Mishkin, 1984). The FEF has been shown to have gain fields for moving targets, and these properties may be able to encode the target position and velocity information (Cassanello, Nihalani, & Ferrera, 2008). Alternatively, the NRTP encodes both saccade and pursuit-related information and could potentially be the key contributor to merging the two pathways in the interceptive saccade and post-saccade pursuit of the moving target. The NRTP could incorporate the moving stimulus's additional position change during the transduction

delay and add this to the movement command downstream in the burst generators via the caudal fastigial nucleus (Goffart & Péliison, 1998). Another theory is that since MT/MST project to the SC, the SC has an additional input to drive the neurons with additional vigor to incorporate the moving target's speed and trajectory, which could compensate for the transduction delay error.

1.3.1 Superior Colliculus Activity for Interceptive Saccades

Only two studies have investigated the SC's neural activity for interceptive saccades, both only using single-unit recordings, comparing the movement field changes for interceptive saccades compared to amplitude-match stationary saccade movement fields. One study concluded their data supported the dual drive hypothesis (Keller et al 1996), and the other supported the remapping activity hypothesis (Goffart et al 2017). More work needs to be completed to determine which hypothesis is the correct mechanism. The goal of this dissertation was to start filling the gaps regarding how the SC population activity changes from the stationary to moving condition.

1.4 Knowledge Gaps and Research Strategies

Main Knowledge Gaps:

- 1) What behavioral metrics change when the oculomotor system drives a saccade to a moving target compared to a stationary target?
- 2) How does target speed and direction affect the interceptive saccade metrics?
- 3) What is the SC's population activity dynamics to drive a saccade to a moving target?
- 4) If the SC population dynamics change between stationary and moving, what information does this tell researchers about how downstream structures encode the SC population activity?

While there has been a plethora of research devoted to understanding the behavior and neural correlates for saccades programmed to stationary targets, the same cannot be stated for saccades to moving targets. There seems to be a lack of consistency and range of target parameters between studies concerning behavior, and the interceptive saccade metrics do not seem to be well defined. Some studies look at only slow speed ranges, while others test fast targets. A few studies tested a small movement range, and others presented different target trajectories, some that are mostly orthogonal to the movement direction. In addition to the trial set-up variability, the results have been varying as well, with some showing significant differences, while others show no difference between stationary and interceptive saccades. The general saccade metrics for interceptive saccades need to be investigated more methodically and intently.

Regarding neural correlations, very little is known about the superior colliculus population activity for interceptive saccades. There is no good understanding of the visual encoding in the SC when a moving stimulus moves across the SC while active fixation occurs. The few studies that have attempted to address this question (Goffart et al., 2017; EL Keller et al., 1996) have done so with single-unit recordings and attempted to understand changes in the SC dynamics through the change in the movement field properties of neurons in the intermediate layers of the SC. Furthermore, there is still an ongoing debate about how the superior colliculus encodes the saccade vector through the population activity, vector averaging, or vector summation. Therefore, developing a technique to drive the SC population into a non-Gaussian distribution will allow for proper testing between the two proposed mechanisms.

In order to address the behavioral metric issues mentioned, we designed our experiments to have a wide range of target speeds (15 – 60°/s) and to intermix both inward (centrifugal) and outward (centripetal) moving targets. We attempted to address previous studies' issues for the

neural activity collection by collecting data with 24-channel laminar electrodes. We collected data from different locations in the SC map and presented the same targets and trial types for each recording. This experimental set-up generated a pseudo-population activity of the SC. As with the behavior paradigm, we compared an extensive movement range, target speed, and different target directions (inward/outward) during the neural activity collection. We hope that these efforts will begin to fill the proposed knowledge gaps for interceptive saccades.

2.0 Behavioral Metrics of Interceptive Saccades in the Rhesus Macaque

2.1 Introduction

High-velocity eye movements, or saccades, are used to direct the visual axis to targets of interest. When a stimulus is stationary, its position informs the eye movement needed to accurately acquire it. However, our environment is dynamic with many moving objects. Additionally, retinal processing imposes a lengthy neural transduction delay of 80-100ms (Becker & Jürgens, 1979). Thus, an eye movement programmed solely on a previously sampled position of a moving stimulus will be inaccurate, and increasingly so with faster target speeds, which would be futile for even mundane tasks like catching a ball. Fortunately, the oculomotor system has evolved to incorporate motion features of an object at different levels (retina, SC/optic tectum, and cortical areas) when producing a saccadic eye movement that visually intercepts it (Cassanello et al., 2008; Leonardo & Meister, 2013; Pélisson, Goffart, Guillaume, Catz, & Raboyeau, 2001).

Research on behavioral, neurophysiological, and clinical aspects of saccades have spanned many decades. Surprisingly, an overwhelming majority of the effort has focused only on saccades to stationary targets, which we will refer to as “stationary saccades”. Far rarer are investigations of saccades to moving targets, which we will denote “interceptive saccades,” although terms like catchup saccades or pursuit saccades have also been used previously. The peak velocity of interceptive saccades has been a focal point of study. The main behavioral result is that interceptive saccades to centrifugal target motions are slower than amplitude-matched saccades to stationary targets (S. de Brouwer et al., 2002; Goffart et al., 2017; EL Keller et al., 1996). There is only one report of an increase in peak velocity of interceptive saccades to targets with centripetal motion

over amplitude-match stationary saccades, but this increase in velocity was meager compared to the overall speed of the movement (Guan et al., 2005). Furthermore, there has not been a concerted effort to explore different target speeds and directions of motion to evoke saccades of different amplitudes. We sought to bridge the gap between previous works by comparing the kinematics of stationary and interceptive saccades across a broad range of target speeds and both centripetal and centrifugal directions.

Stationary saccades fall on the “main sequence”, exhibiting a saturating exponential relationship between amplitude and peak velocity and a linear relationship between amplitude and duration. We observed the same qualitative pattern for interceptive saccades for both inward and outward radial target motion and, most interestingly, the attenuation was strongest for medium target speeds compared to amplitude-matched interceptive saccades for slow or fast target speeds. These results are interpreted through a conceptual framework in which integration of target motion in the superior colliculus, a subcortical structure central for saccade generation, is speed-dependent and most effective in a limited target speed range.

2.2 Methods

General and Surgical Procedures

Four adolescent rhesus macaques (*macaca mulatta*; three males, one female, ages: 5-10 years) were trained to make saccades to stationary and moving targets. The experimental procedures were conducted on Institutional Animal Care and Use Committee approved protocols at the University of Pittsburgh. Protocols also complied with Public Health Service policy and Human Care and Use of Laboratory Animals guidelines. As these animals were used in previous or concurrent

neurophysiological studies, they also underwent surgical procedures in an aseptic environment. They were fitted with a Teflon-coated stainless-steel wire around the eye to measure gaze position with the magnetic induction method, a head post to restrain the head during experiments, and/or a cylindrical chamber over a craniotomy to perform neurophysiological recordings. In some animals, eye movements were measured with a non-invasive infrared eye-tracking system (Eyelink 1000plus, SR Research) and head-restraint was achieved with a custom-fit thermoplastic mask (CIVCO Medical Solutions) (Drucker, Carlson, Toda, DeWind, & Platt, 2015).

Visual Stimuli and Behavior

An LED-backlit flat screen television was used to present green squares of 4x4 pixels on a dark gray background and measured to subtend approximately 0.5° of visual angle. Eye position was sampled at 1 kHz for both scleral search coil and eye tracking techniques. Data acquisition was performed with a real-time LabView-based controller interface (Bryant & Gandhi, 2005).

For this study, all animals were trained to direct saccades to stationary or moving targets. Every trial began with the presentation of a central target, which the animal was required to fixation for 300-500ms. Next, a target appeared in the visual field and either remained stationary or began to move at a constant velocity. The central target remained illuminated for an additional 0-1200 msec (delay period), during which time fixation remained directed to it. The offset of the central target cued the animal to make a saccade to the peripheral target within 500ms for stationary targets or 400-700ms for moving targets (see below for justification). A liquid reward was administered if the animal correctly shifted its gaze to the peripheral target and maintained fixation for 100-800ms. If the animal broke fixation by deviating its gaze outside a 3-deg radius around the central

target before it was extinguished, or if the animal did not make a saccade in the time allotted, the trial was aborted. Figure 1 shows a schematic of the steps in a moving target trial.

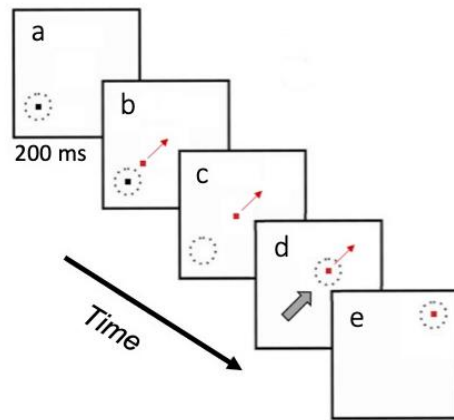


Figure 1: Delay Saccade Task for an Outward Moving Target

A) The subject began the trial by fixating on a stationary fixation target (black, T0). The dashed circle denotes the subject's gaze. B) After 100-1200ms, a peripheral moving target (red, T1) was presented (red arrow denotes target displacement), while the subject maintained fixation on T0. C) The animal received the go cue when T0 was extinguished. D) The animal made a saccade to T1 (grey arrow denotes the saccade vector). E) After intercepting T1, the subject pursued T1 for a variable amount of time to successfully complete the trial and receive a liquid reward.

For moving target trials, the speed of the moving target was different for the four subjects mainly because some of the data were collected in previous experiments (subjects BB and WM) (Goffart et al., 2017), while other data were collected specifically for this study (subjects BU and BL). Each animal experienced three (low-medium-high) different target speeds (BB: 10-20-30°/s; Monkey WM: 20-40-60°/s; BU and BL: 15-30-45°/s) for inward and outward moving targets, and these speeds were randomly interleaved with stationary targets.

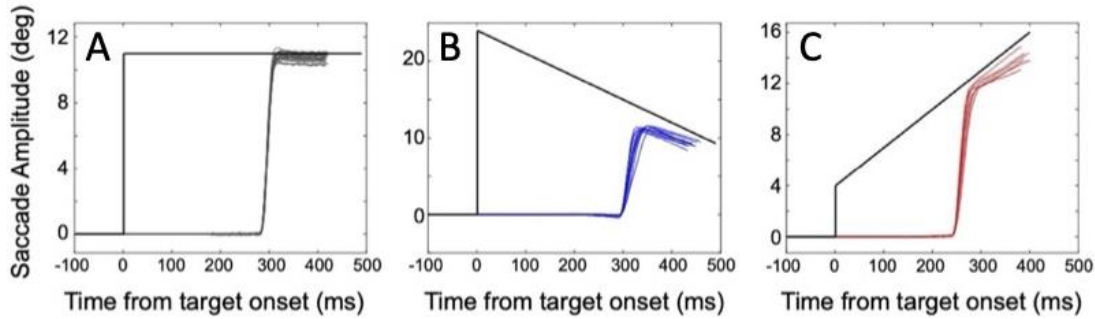


Figure 2: Amplitude-Matched Saccade Profiles for Static and Moving Targets

Movements to stationary (A), inward-moving (B), and outward-moving (C) targets. The data are $11^{\circ} \pm 1^{\circ}$ movements from subject BU. The position of the target relative to the subject's initial fixation during the trials is plotted in black for all three panels. The speed of the moving target is 30 deg/s for panels B and C.

The moving targets had only radial trajectories on the screen, moving inward or outward relative to the fixation target (see Figure 2 for example eye movement traces). The starting target position as well as its speed and direction of motion were randomly chosen but confined along the cardinal and intercardinal axes (see Figure 3A). To capture larger movements, especially for fast moving targets, the fixation target was moved from the center of the screen, which allowed larger target displacement on the screen. In addition, the subjects were required to make a saccade within a grace period (400-700ms after the go-cue) to prevent the moving target from going off-screen (outward) or colliding with the fixation target (inward). In the case of an inward target, the target gets closer to fixation with time, and one observed strategy was the willingness to wait for the moving target to come to the subject's fixation position. Waiting for the target to reach current fixation could induce only pursuit and not require an interceptive saccade which would not be utilized in this study. The grace period ensured the subject performed the trial correctly and did not wait too long. Saccades were measured with a 30%/s onset/offset criterion. Each saccade was visually inspected, and their onset/offset was manually adjusted as necessary.

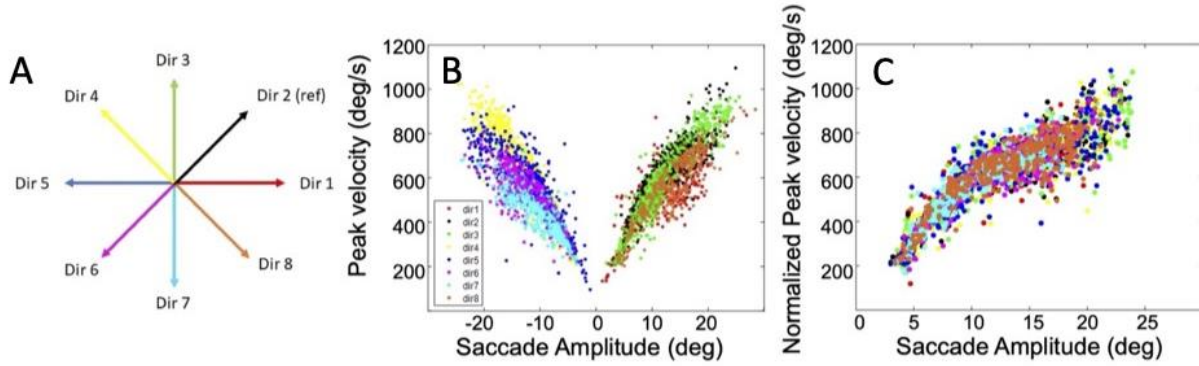


Figure 3: Session Combining Method

A) A diagram of the eight directions, spaced 45 degrees apart, that were tested for each subject. B) A plot of peak velocity of saccades made to stationary targets along each direction (colors in B match the directional line in panel A) plotted against saccade amplitude. Negative amplitudes indicate leftward or downward movements, while positive indicate rightward and upward movements. C) All stationary peak velocity data were normalized to Direction 2 (black in panel A) and plotted, overlapping each other. Since the stationary points are the control for the results, the median and standard deviation for each direction is normalized to be the same across the movement directions.

Combining Data for Each Subject

The sparsity of data for any individual movement direction (8 movement directions shown in Figure 3A) made it difficult to compare stationary and interceptive saccades across a large range of movement sizes. Therefore, we combined data from all movement axes onto one axis by normalizing the control (stationary) data from each movement axis (Figure 3B and 3C shows the peak velocity normalization, but this was done for all metrics). To combine each saccade metric, we computed a 25-point moving-window median and standard deviation for all stationary and interceptive saccade metrics on each movement axis. Then, we designated one of the movement directions to be the reference direction, and rotated the other movement axes to the reference axis. To pool the stationary data, we subtracted the median from movements collected in each individual direction (stat_median) and then divided by the standard deviation calculated in each direction (stat_std). Then, we multiplied with the standard deviation in the reference direction (Ref_std) and

added the reference direction median (*Ref_median*). To pool interceptive saccade data from difference movement directions, we used Equation 2-1. We used the same process for the interceptive saccade movements as we did with the stationary movement except, instead of using the interceptive median and standard deviation for the interceptive movements, we utilized the median and standard deviation of the stationary movements along each specific movement direction. This was a crucial detail in our analysis because we wanted to maintain the differences between stationary and interceptive saccade movements along each movement direction.

$$intrcpt_norm_i = \frac{Ref_{std}}{stat_{std}} * (intrcpt_i - stat_{median}) + Ref_{median} \quad (2-1)$$

intrcpt_norm - normalized values of the interceptive saccades on the rotating axis
stat - values calculated from the stationary movements along the rotating axis
Ref - values calculated from the stationary movements along the reference axis
i - denotes separate movements computed within the 25-pt movement bin
median - median of the movements calculated from 25-pt movement bin
std - standard deviation of the movements from 25-pt movement bin

Peak Velocity Attenuation

To compute and analyze the change in peak velocity for interceptive saccades relative to stationary saccades, we computed a metric termed peak velocity attenuation (see Equation 2-2). Since we desired to compare changes in peak velocity across subjects, we utilized the peak velocity attenuation metric, as it normalizes the interceptive saccade peak velocity by the stationary saccade peak velocity. To be explicit, peak velocity attenuation was calculated by taking the difference between each interceptive saccade peak velocity and the average peak velocity of the 25-closest (according to amplitude) stationary saccades, and then divided by average peak velocity of the 25-

closest stationary saccades. Peak velocity attenuation will be zero if the moving and stationary trials are matched. The peak velocity attenuation will be positive if the interceptive saccades are slower than the stationary saccades and negative if the interceptive saccades are faster than the stationary. The normalization step permits comparison of peak velocity attenuation across subjects.

$$PkV \text{ Attenuation} = \frac{(\overline{PkV}_{stationary} - PkV_{moving})}{\overline{PkV}_{stationary}} \quad (2-2)$$

\overline{PkV}_{moving} - peak velocity of an interceptive movement
 $\overline{PkV}_{stationary}$ - "closest 25-pt" average peak velocity for stationary movements

Statistical Analysis

In Figures 4, 6-8, the bold traces represent the means of the stationary (black), outward (red), and inward (blue) distributions for different metrics across the saccade amplitude ranges that were collected. The mean was calculated for bins with four or more movements. If a bin did not exceed four movements, the mean value for that bin was interpolated between the neighboring closest means on either side of that bin. The dashed lines that surround the mean values represent the 95% confidence interval for the mean. Statistical significance was determined by comparing saccade metrics within 1-degree amplitude bins. Within each bin, if the number of movements per bin for all three trial types exceeded 10 movements each, a one-way ANOVA ($\alpha=0.05/3$) was conducted, and if the null hypothesis was rejected, a post-hoc Tukey-Kramer HSD test ($\alpha=0.05/3$) was used to determine the significance difference between the groups. The significance was noted in the color bar at the bottom of each graph. The blue color bar indicated a significant difference between

inward and stationary movements, the red color bar indicated significance between outward and stationary movements, and the purple bar indicated a significance difference between inward and outward movements for that 1-degree bin. If the null hypothesis was not rejected in the one-way ANOVA, then all three bars were colored gray. If there were not enough points for both of the interceptive saccade types (10 movements each), then there was no color plotted, as no statistical test was conducted. If there were enough movements for one of the interceptive saccade trial types but not the other, a Bonferroni-corrected t-test ($\alpha=0.05/3$) was conducted between the interceptive saccade movements that had enough points (10 or greater) and the stationary movements for that bin. For Figures 5, 9, and 10, one-way ANOVA tests were utilized to determine if significance existed across the different target speeds for each subject separately. Target direction (outward/inward) was tested separately for this analysis. If the null hypothesis was rejected in the one-ANOVA, a post-hoc Tukey-Kramer HSD test ($\alpha=0.05/3$) was used to determine the strength of significance between conditions for data sets that had a null stationary distribution (Figures 5 & 9). There was no post-saccadic pursuit for stationary trials, so we could not test the strength of the significance for post-saccadic pursuit gain, but we could determine if differences existed in the post-saccadic pursuit speed across different target speeds within each subject (one-way ANOVA, $\alpha=0.05/3$, F-statistics relayed in the text).

2.3 Results

There is relatively little known about the behavior of saccades that catch moving targets, but there is a well-developed understanding of the behavioral dynamics of saccades directed to stationary targets (stationary saccades) (Leigh & Zee, 2015). Therefore, the goal of this study was to demonstrate how moving target speed and moving target direction (radially inward or radially outward, relative to center of gaze) affect the kinematics of interceptive saccades and to compare them to features of stationary saccades. We measured the similarities and differences in the main sequence of interceptive and stationary saccades. The main sequence of saccades refers to the quasi-linear, stereotypical relationship between the peak velocity and the duration of saccades across a large range of saccade amplitudes, as originally described by Bahill et al. (1975). In addition to the main sequence, saccade latency, saccadic error, and pursuit gain were compared across the different target speeds and target directions, as these saccade metrics may be affected by programming a saccade to a moving target.

Figure 4 illustrates the mean peak velocity with 95% confidence intervals of saccades to stationary (black) and moving targets (blue – inward, red – outward) as a function of saccade amplitude. The analysis is shown for four animals (rows) and three different speeds for each animal (columns). Monkeys BL and BU had the same target speed range (15, 30, and 45 deg/s), monkey WM had a slightly larger target speed range (20, 40, and 60 deg/s), and monkey BB had a slightly smaller range (10, 20, and 30 deg/s). Thus, the slow, medium and fast are labels to rank speeds observed by each animal, not across all of them. The number of movements utilized for each subject, trial type, and target speed is noted in Table 1 (“Total” column). In majority of our subjects, with the exception of subject BL, the peak velocity of interceptive saccade was consistently and significantly slower than the peak velocity of stationary saccades for the majority

of the amplitude range (one-ANOVA with post-hoc Tukey-Kramer HSD test ($\alpha=0.05/3$), see Figure 4). Notably, the attenuation in peak velocity occurred for interceptive saccades directed to both inward and outward target motions. This attenuation in interceptive saccade peak velocity has been documented previously for outward target motion (Goffart et al., 2017; Guan et al., 2005; EL Keller et al., 1996), but not for inward motion to the best of our knowledge.

Table 1: Number of Movements Collected for Each Trial Type

	Total				10° ± 2°			
	Stationary	Slow	Medium	Fast	Stationary	Slow	Medium	Fast
WM	1058	234, 328	276, 475	162, 307	217	47, 76	61, 113	45, 69
BU	4832	2281, 1844	1689, 1293	643, 432	1573	889, 892	880, 497	227, 130
BL	1172	352, 249	166, 171	108, 103	209	134, 125	63, 62	69, 38
BB	1539	311, 194	571, 432	154, 148	323	126, 157	188, 196	45, 63

The number of movements used for each condition in Figures 4, 6, 7 and 8 is shown in the “Total” section of the table. The inward trial count displayed in blue, and the outward trial count displayed in red. The other section “10° ± 2°” reports the number of movements included in the analyses shown in Figures 5, 9, and 10

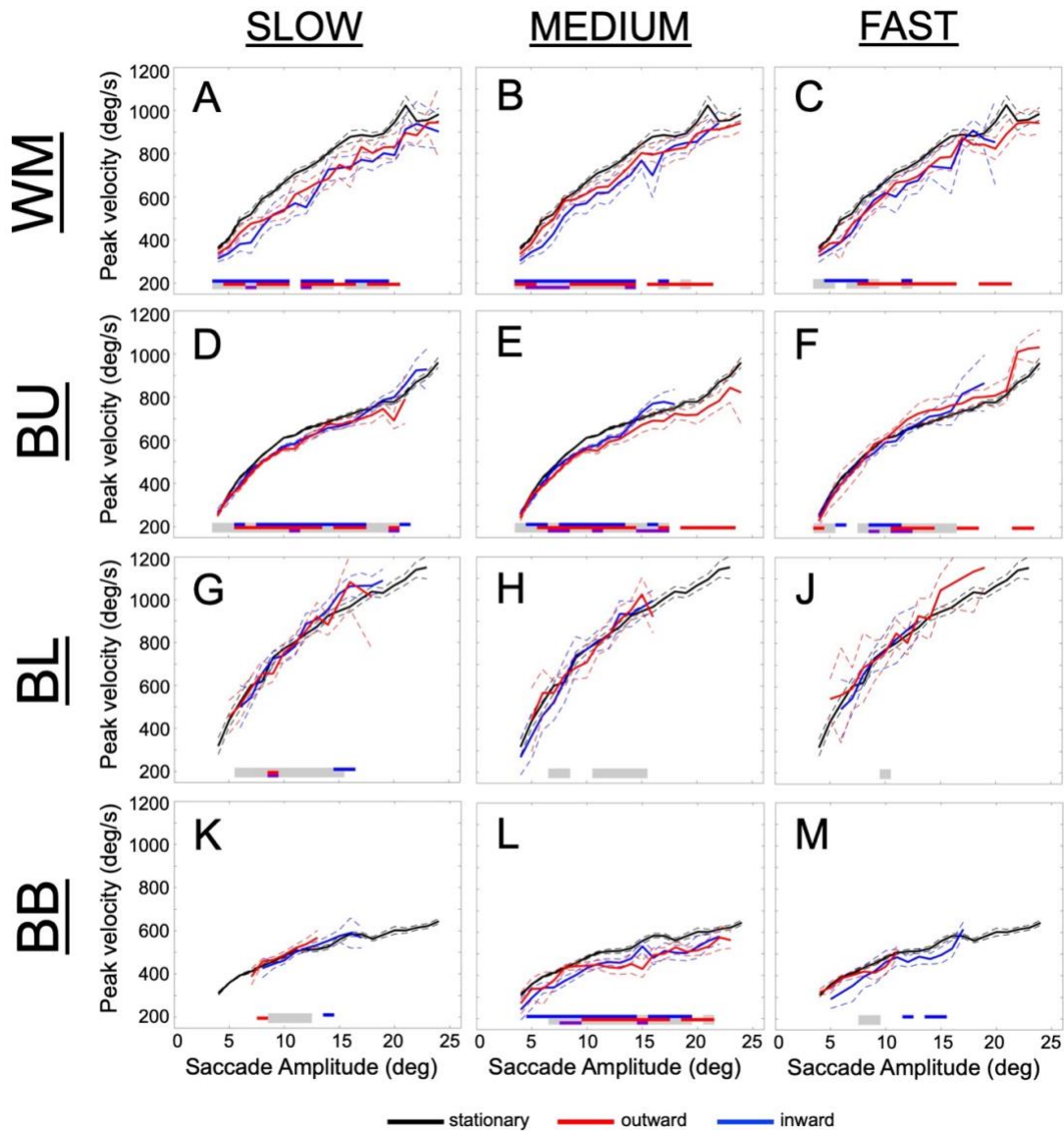


Figure 4: Main Sequence Comparison Between Moving and Stationary Trials

Each row is a different subject (BB, BL, BU, WM). Adjusted saccade peak velocity was plotted against saccade amplitude for each animal for each speed (see details in Methods). The plots directly compare the mean (bold trace) and 95% confidence interval (dashed lines) for the peak velocity of saccades to stationary targets (black), inward moving targets (blue), and outward moving targets (red). The significance ticks at the bottom of each plot denote a significant difference between the interceptive and stationary movements in a 1-deg bin (one-way ANOVA, with post-hoc Tukey-Kramer HSD, $p < 0.05/3$). Significance was indicated as a blue tic for the stationary-inward comparison, a red tic for the stationary-outward comparison, and a purple tic for the inward-outward comparison. The gray ticks indicate non-significant differences between comparisons. Any blanks in the significance ticks would indicate there was not enough movements in that bin to complete the statistical test (minimum of 10 movements).

To investigate the effect of target speed on interceptive saccades, we calculated the attenuation in peak velocity for each subject for saccades $10^\circ \pm 2^\circ$ in amplitude (see methods). The number of movements utilized for each subject, trial type, and target speed is noted in Table 1 (“ $10^\circ \pm 2^\circ$ ” column). Figure 5 plots mean and 95% confidence interval of the attenuation metric (see Methods) as a function of target speed. Three of the four animals (exception: monkey BL) collectively exhibited a converging effect of target speed on peak velocity of interceptive saccades. The attenuation was substantial and significant for medium range speeds but was minimal or negligible for slow (10 deg/s) and fast (>40 deg/s) speeds (Figure 5). This effect was present for both outward and inward target motions but was more prominent for the inward condition. For outward moving targets, statistical differences were determined by one-way ANOVA (BU:F(3,2447)=213.182,p \rightarrow 0; BL:F(3,1203)=8.018,p \rightarrow 0; BB:F(3,1410)=78.846,p \rightarrow 0; WM:F(3,1132)=253.508,p \rightarrow 0), and strength of significance was determined through a post-hoc Tukey-Kramer HSD test ($\alpha=0.05/3$) and marked with an asterisk in Figure 5A. Likewise, inward interceptive movements had statistical significance determined through one-way ANOVA (BU:F(3,2775)=118.146,p \rightarrow 0; BL:F(3,1238)=1.3596,p=0.251; BB:F(3,1347)=148.111,p \rightarrow 0; WM:F(3,1061)=369.714,p \rightarrow 0) and a post-hoc Tukey-Kramer HSD test ($\alpha=0.05/3$) and noted with an asterisk in Figure 5B.

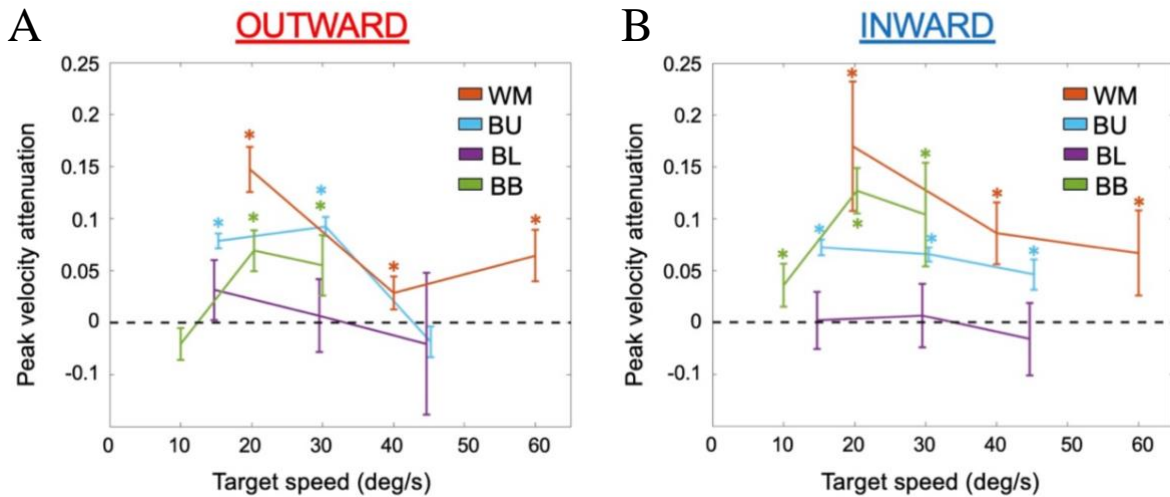


Figure 5: The Attenuation of Peak Velocity for Interceptive Saccades

Peak velocity attenuation was calculated for movements of $10^\circ \pm 2^\circ$ amplitude as a function of target speed. Attenuation was computed for both A) outward and B) inward moving targets. Each data point denotes the mean with 95% confidence bars and each color represents a subject. The asterisks denote significance from a stationary null distribution according to a one-way ANOVA with Tukey-Kramer HSD post-hoc test ($P < 0.05/3$).

Saccades to stationary targets exhibit a linear relationship between amplitude and duration. After combining the durations across the movement directions, the same relationship was also observed for interceptive saccades for all target speeds and target directions (Figure 6). We expected longer saccade durations to compensate for the attenuation in peak velocity. The prevalence of red and blue colors on the horizontal bands, which denote statistical difference (one-ANOVA with post-hoc Tukey-Kramer HSD test ($\alpha=0.05/3$) between the moving and stationary conditions in each panel, supports our prediction. For the subjects that showed a change in the duration for interceptive movement (subjects WM, BU, and BB) the increase in duration was greatest for target speeds between 20-30 deg/s (Figure 6 A,E,L). Monkey BL had little to no

difference in saccade duration between interceptive and stationary saccades, with no consistent significance across the saccade amplitude ranges collected (Figure 6 G,H,J).

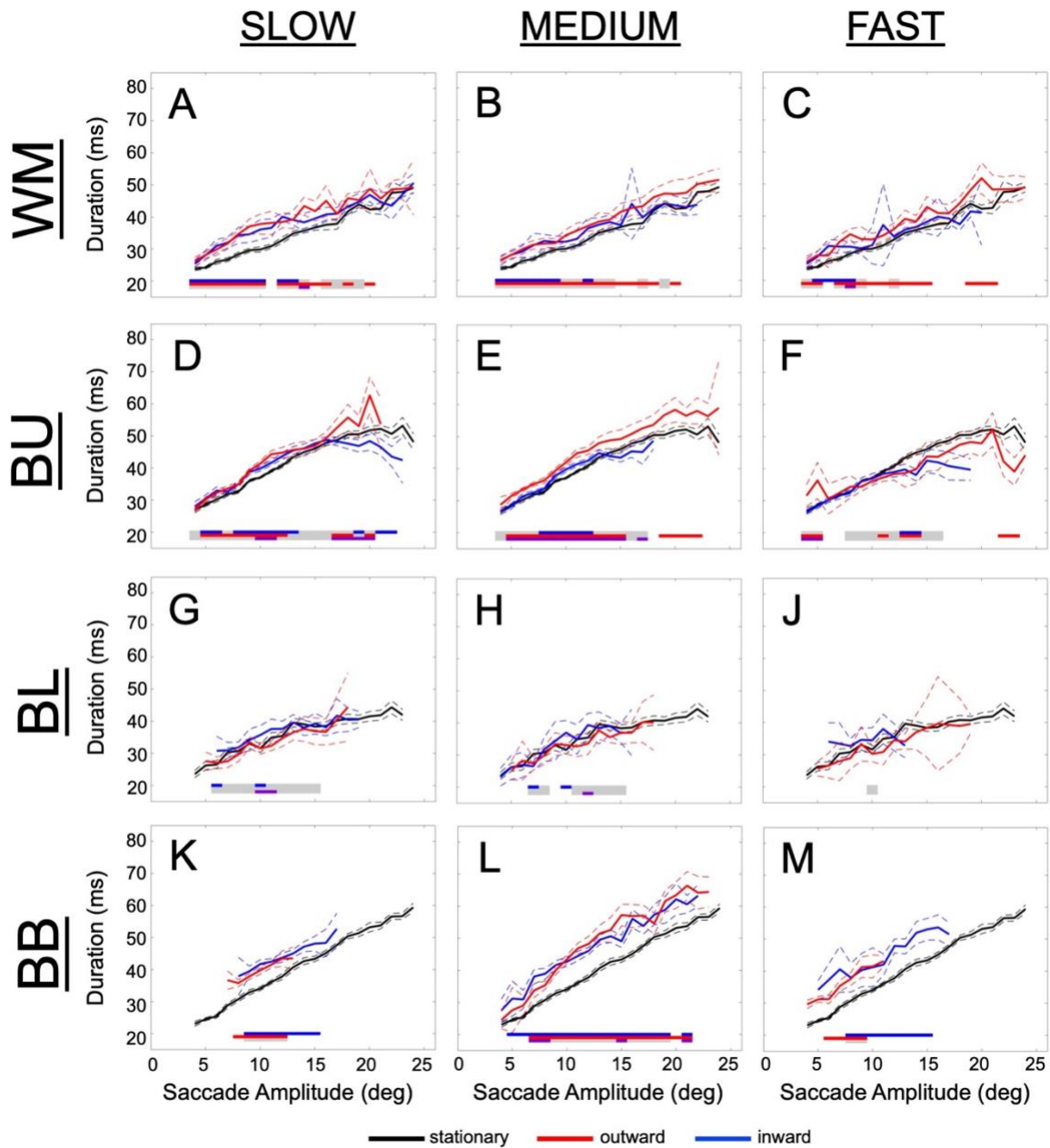


Figure 6: Saccade Duration Comparison Between Moving and Stationary Trials

Each row is a different subject (BB, BL, BU, WM). Adjusted saccade duration was plotted against saccade amplitude for each animal for each speed in separate columns (similar to Figure 4). The plots directly compare the mean (bold trace) and 95% confidence interval (dashed lines) for the duration of saccades to stationary targets (black), inward moving targets (blue), and outward moving targets (red). The significance ticks and colors at the bottom of each plot follow the convention used for Figure 4.

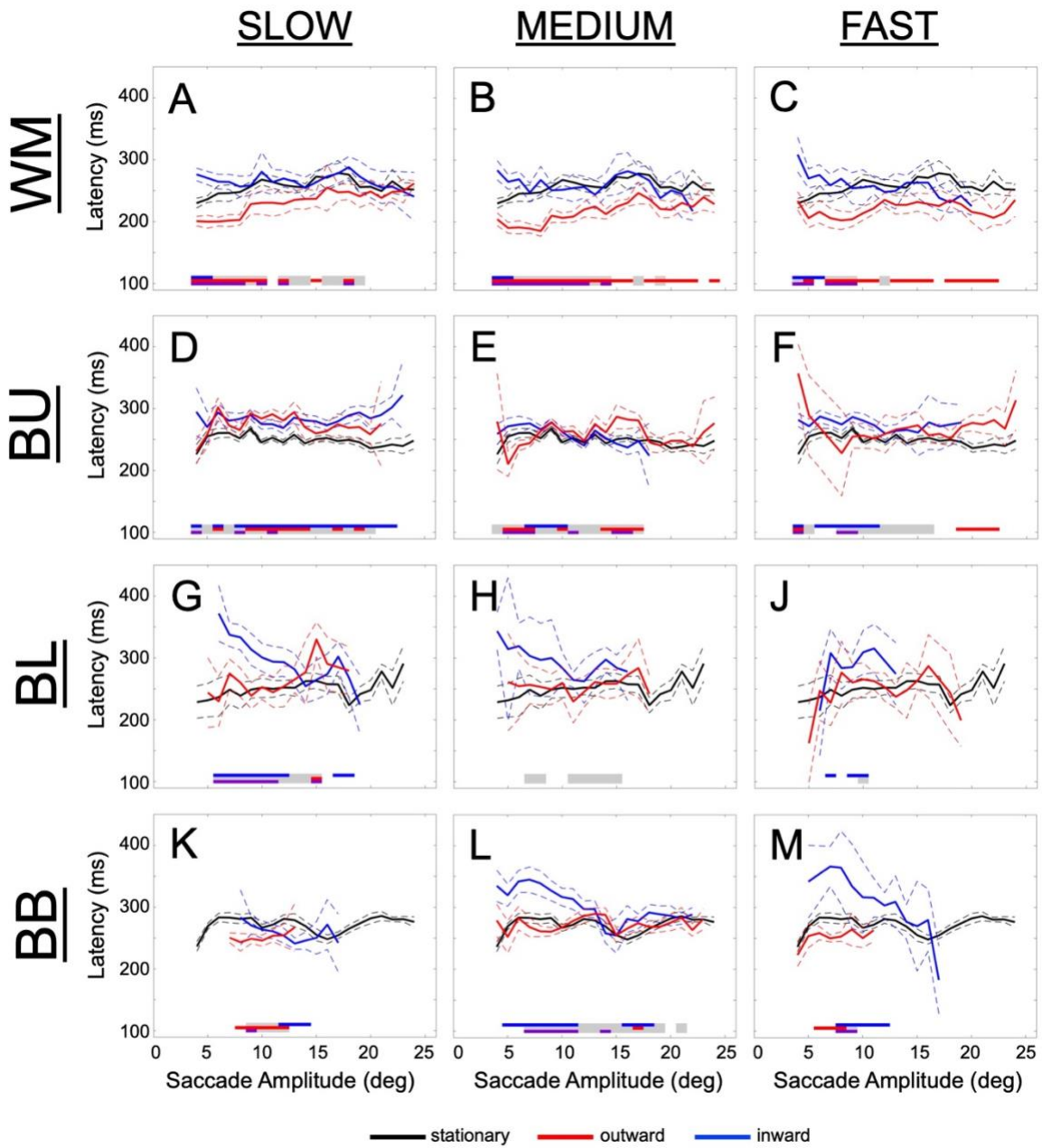


Figure 7: Saccade Latency Comparison Between Moving and Stationary Trials

Each row is a different subject (BB, BL, BU, WM). Normalized saccade latency was plotted against saccade amplitude for each animal for each speed (similar to Figure 4 & 6).

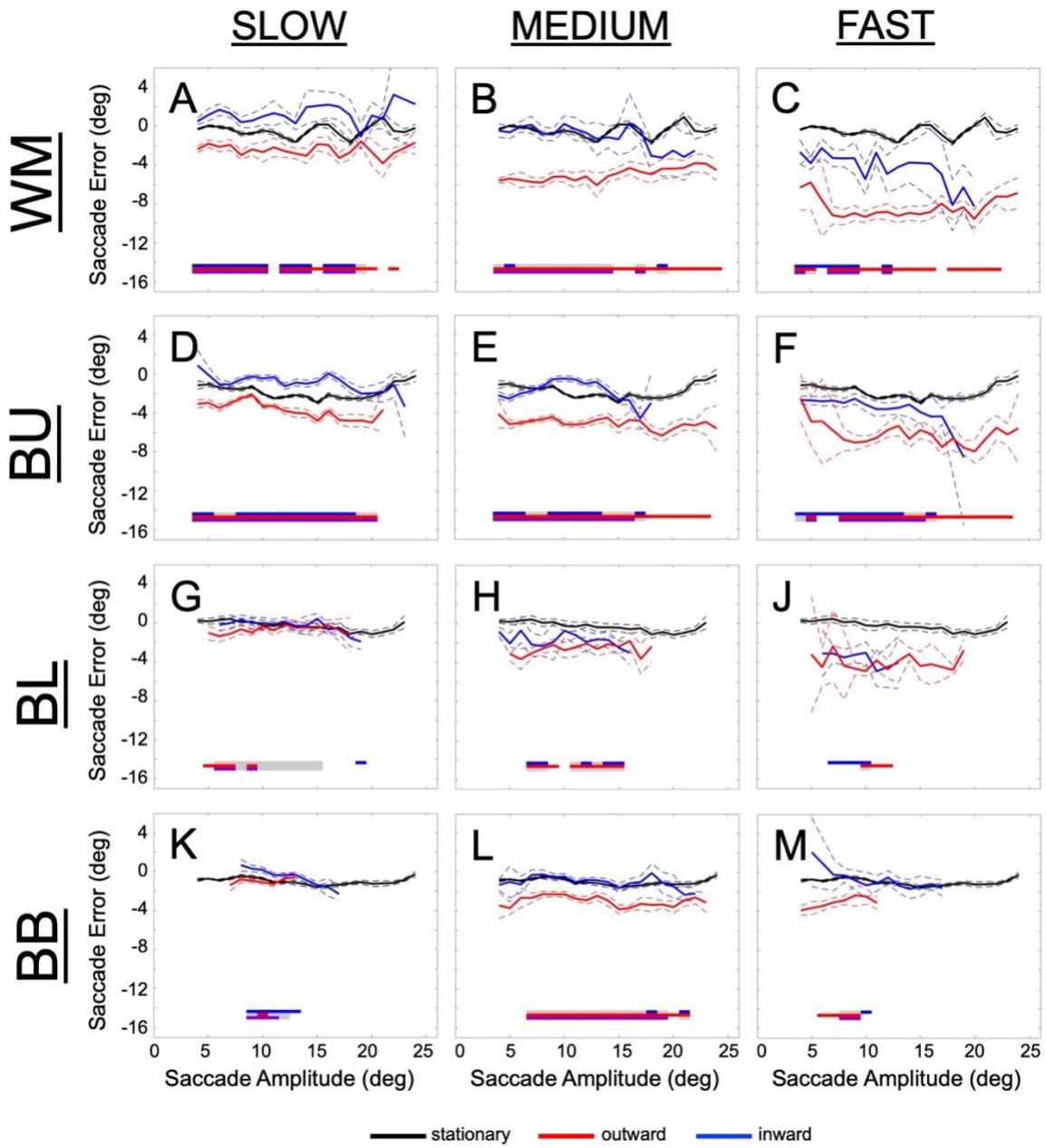


Figure 8: Saccade Error Comparison Between Moving and Stationary Trials.

Each row is a different subject (BB, BL, BU, WM). Normalized saccade error was plotted against saccade amplitude for each animal for each speed (similar to Figure 4, 6 & 7).

We also compared the latencies of both types of movements across a range of saccade amplitudes (Figure 7). Based on the patterns of red and blue horizontal bands across the panels, we found idiosyncratic patterns both across and within animals. For monkey WM, the inward latencies match stationary latencies, but outward saccade latencies were significantly shorter for most saccade amplitudes (one-ANOVA with post-hoc Tukey-Kramer HSD test ($\alpha=0.05/3$)). Monkey BB had increased latency for inward interceptive saccades, but decreased latency for outward saccade latency, especially at small saccade amplitudes (one-ANOVA with post-hoc Tukey-Kramer HSD test ($\alpha=0.05/3$)). For the most part monkeys BU and WM had consistent interceptive saccades latencies across saccade amplitudes, but for monkeys BL and BB, they had a significant increase in saccade latency for inward interceptive saccades at small saccade amplitudes.

Figure 8 illustrates the relationship between saccade amplitude and saccade error, or the vectorial distance between the eye position and the target position at the end of the interceptive saccade. As before, the horizontal bands denote whether the means of the error distributions in 1-deg bin are significantly different from the stationary condition. Positive and negative errors for stationary saccades represent hypermetric and hypometric movements, respectively. In a moving target trial, positive error indicates the eye-position at saccade-end is ahead of where the moving target is going to be. Similarly, a negative error for an interceptive saccade indicates the eye-position is behind where the target is moving. Importantly, this convention requires that the error sign is switched for inward target motion compared to stationary and outward target motion conditions. For nearly every animal and target speed, the endpoint error for outward target motion was significantly different from the stationary condition. The error was hypometric and increasingly so for faster target speeds. For inward trials with slower target speeds, most monkeys

showed a positive error, which means the animal made a shorter saccade as the target approached fixation (Figure 8 A, D, G, J). At faster speeds, some animals showed a negative error meaning the animal made a larger saccade than necessary for these similar sized movements. Monkey WM showed the largest error for moving targets and was the most affected by the speed of the target, as monkey WM was not very good at intercepting very fast-moving targets, with almost 10 deg error for outward moving targets across all measured saccade amplitudes.

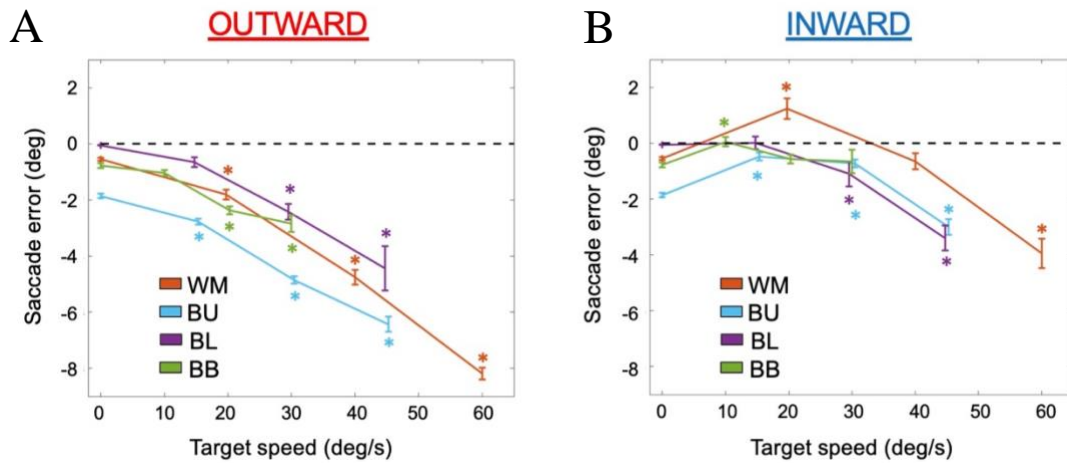


Figure 9: Saccadic Error as a Function of Target Speed

The saccadic error for each animal was calculated for $10^\circ \pm 2^\circ$ amplitude movements, as a function of target speed. Error was computed for both A) outward moving targets and B) inward moving targets. Saccades to stationary targets are plotted at 0 deg/s. The different colors correspond to the different subjects, with the mean and 95% confidence intervals plotted for each condition. The asterisks denote significance from a multiple comparison analysis ($P < 0.05/3$).

To better compare saccade error across speed, we pooled all $10^\circ \pm 2^\circ$ saccades for each subject and plotted the mean saccade error as a function of target speed (Figure 9). The error associated with stationary targets trials is mapped to 0 deg/s. For outward moving targets, the error for $10^\circ \pm 2^\circ$ saccades become increasingly hypometric with target speed. For inward target

motion, the error becomes more positive as slow speeds, indicating that eye position at saccade end is leading the target. As target speed increases, however, the error become hypometric and the eye lags inward moving targets too. One-way ANOVA was used to determine statistical significance, and a post-hoc Tukey-Kramer HSD test ($\alpha=0.05/3$) to confirm the strength of the differences between error across conditions for each animal denoted with an asterisk ($P<0.001$) for both outward trials (BU:F(3,2974)=769.685, $p\rightarrow 0$; BL:F(3,403)=110.928, $p\rightarrow 0$; BB:F(3,734)=225.873, $p\rightarrow 0$; WM:F(3,458)=1211.70, $p\rightarrow 0$) and inward trials (BU:F(3,3305)=186.689, $p\rightarrow 0$; BL:F(3,437)=78.894, $p\rightarrow 0$; BB:F(3,671)=24.218, $p\rightarrow 0$; WM:F(3,388)=139.386, $p\rightarrow 0$).

While saccade error marks the positional encoding error, we were also interested in understanding the velocity encoding error, or how well the subject is able to encode the velocity of the target prior to interceptive saccade. One way to estimate the velocity encoding error is by measuring the smooth pursuit that directly follows the interceptive saccade, or post-saccadic pursuit (PSP). We measured PSP by averaging the velocity achieved over 30-80 milliseconds after interceptive saccade offset. This 50ms window is a reasonable time frame to measure velocity encoding prior to the saccade because it is long enough after the saccade to not be influenced by any deceleration effects from the saccade, yet it also occurs during the “open-loop” period before visual reafference can modify pursuit (Lisberger et al., 1987). We computed a one-way ANOVA to determine statistical significance in post-saccadic pursuit gain across moving trial conditions for each subject for outward moving trials (BU:F(2,1336)=43.071, $p\rightarrow 0$; BL:F(2,173)=2.144, $p=0.120$; BB:F(2,411)=12.644, $p=4.687e^{-6}$; WM:F(2,118)=14.335, $p\rightarrow 0$), and inward moving trials (BU:F(2,1720)=13.583, $p\rightarrow 0$; BL:F(2,230)=1.220, $p=0.297$, BB:F(2,334)=1.7886, $p=0.169$, WM:F(2,63)=11.438, $p=5.783e^{-5}$). There are two main takeaways

from our pursuit analysis. First, for outward moving target trials the PSP decreases overall for all subjects as target speed increases. This result was supported by de Brouwer et al. (2001). Second, inward moving target trials did not have as much of a target speed effect, as two subjects showed no significant change in PSP as a function of target speed (Figure 10B, subjects BL & BU).

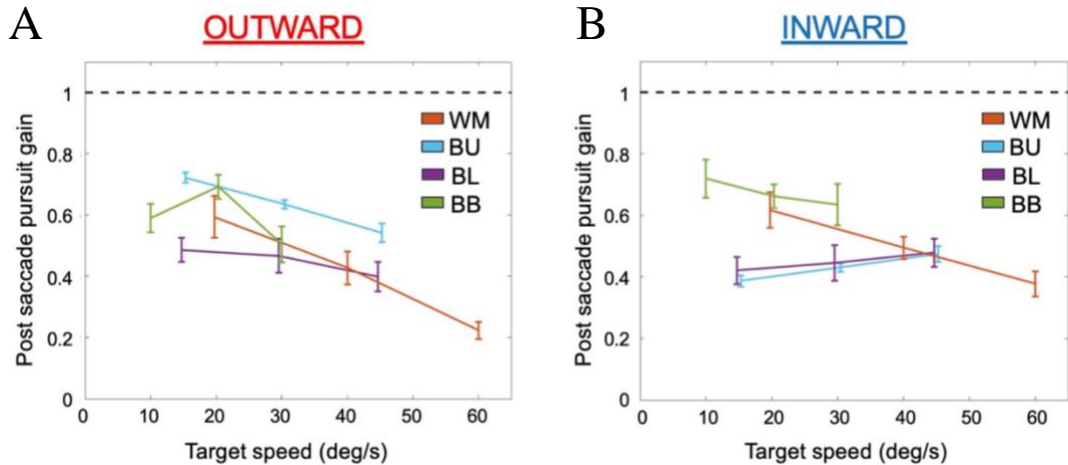


Figure 10: Average Pursuit Gain for Interceptive Movements

The average pursuit was calculated for $10^\circ \pm 2^\circ$ amplitude movements across target speeds for each subject. The post-saccadic pursuit gain was plotted for both A) outward moving targets or B) inward moving targets. The average was computed over a 50ms window, 30ms after the interceptive saccade had ended. The different colors correspond to the different subjects, with the mean and 95% confidence intervals plotted for each condition.

2.4 Discussion

Saccades are essential to survival as these movements help to bring our line of sight onto moving objects in our dynamic surroundings (Leigh and Zee 2015). Visual information about a subject's environment is attained through saccades, so when a new moving stimulus comes into

the field of view, the subject must drive a saccade to the moving target to identify it. To program an interceptive saccade, the subject must estimate the position of the target to drive the saccade to by anticipating the future path of the target. Anticipating the target trajectory is crucial to accurately catching the moving target, due to the inherent neural transduction delay (80-100ms) prior to the saccade. Building an internal model of the target's trajectory allows the oculomotor system to compensate for how much space the target will traverse during the transduction delay (Becker & Jürgens, 1979; Fleuriet et al., 2011; Schlag & Schlag-Rey, 2002). Both humans and non-human primates compensate for this delay and intercept moving targets accurately (S. de Brouwer et al., 2002; Eggert et al., 2005; E Keller & Johnsen, 1990). While it is known that interceptive saccades can be accurate, very little is known about the kinematics of these movements.

Previous Studies of Interceptive Saccades

Saccade metrics for movements to stationary targets are well known and characterized (Bahill et al., 1975; Leigh & Zee, 2015; Robinson, 1973; Westheimer, 1954), while interceptive saccades have been poorly studied and are not well understood. Fuchs (1967) demonstrated that, like humans, non-human primates were able to perform saccades to moving targets and that the movements looked qualitatively similar to humans, with the key differences that monkey saccades were much more rapid, reaching a higher peak velocity, and that monkeys can pursuit much faster to moving targets than humans (Fuchs, 1967). A few studies also evaluated “catchup” saccades produced during initial and sustained phases of smooth pursuit (S. de Brouwer et al., 2002; Kim, Thaker, Ross, & Medoff, 1997; Ron, Vieville, & Droulez, 1989). De Brower et al. (2002) reported several of the same differences between stationary and catchup saccades that are reported between stationary and interceptive saccades in this study, such as slower interceptive saccades and higher

error with higher speeds. It is difficult to directly compare the stationary and the moving conditions since the range of movements did not match. In addition, an issue with having the animal initially pursuit is that the saccade amplitude had to be estimated by subtracting off the pursuit velocity during the saccade.

To focus the understanding on the interceptive saccade, and less so on the effect pursuit may have on the saccade, future studies were designed to start with an initial fixation prior to saccade, which we refer to as an interceptive saccade (Goffart et al., 2017). Keller et al. (1996), who used fast target speeds (40-60 deg/s) and only outward (away from fixation) target direction, noted that interceptive saccades had a significant decrease in peak velocity relative to saccades made to amplitude-matched stationary saccades. To investigate the dynamics of the saccade, and compare the velocity traces of the interceptive movements to stationary, Eggert et al. (2005) attempted to investigate the dynamics of interceptive saccades to inward and outward (centripetal and centrifugal) moving targets, and found that peak velocity decreased for saccades to outward moving targets, but increased for saccades to inward moving targets. Unfortunately, they only used a narrow set of parameters to understand the dynamics: one speed (10 deg/s) and one movement size (~6 degrees). To separate position from velocity information in the interceptive saccade programming, Flueriet and Goffart (2011) studied interceptive saccades that intercept moving targets that have a trajectory that was mostly orthogonal to the saccadic movement, and tested a target speeds of 7, 14, and 21 deg/s. Their main behavioral results were longer latencies and saccade error that increased with target speed, similar to what was found in this study. Although there was no statistical comparison of saccade kinematics between interceptive and stationary saccades, there appeared to be no distinct difference in the peak velocity of saccades made to stationary and moving targets.

Speed-dependent modulation of main sequence for interceptive saccades

The goal of this study was to understand the kinematics of saccadic eye movements to moving targets. Previous work has measured limited target parameter ranges and sparse aspects of the behavior for interceptive saccade movements. This study provides a broader perspective of how target parameters drive certain behaviors in interceptive movements. The peak velocity of interceptive saccades may be more idiosyncratic than previously reported. The main takeaway from our results is that most subjects have pronounced attenuation in their interceptive saccade peak velocity, and although the amount of attenuation varied greatly between the four subjects, there seems to be a speed-dependent modulation of peak velocity attenuation (see Figure 5). There is a distinct inverted-U trend in the amount of peak velocity attenuation as function of target speed, and we hypothesize that this comes as a function of the subject's ability to internally model the trajectory of the moving stimulus.

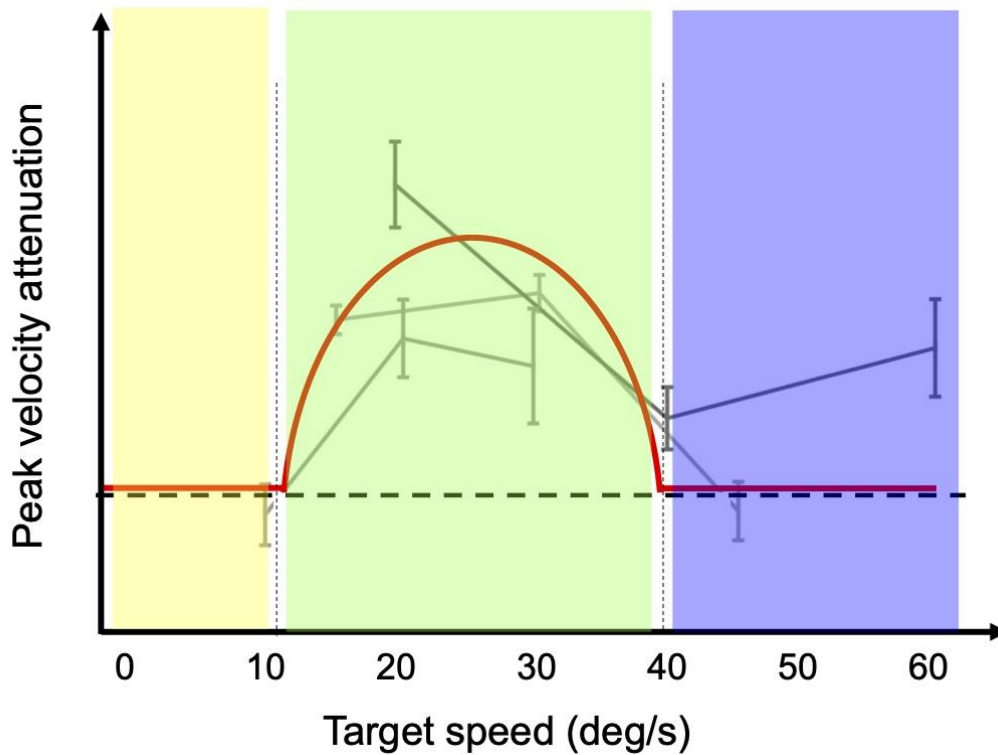


Figure 11: Peak Velocity Attenuation Pattern Across Subjects

The general trend (red trace) in the peak velocity attenuation across the 3 subjects (subjects WM, BU, BB) that had a significant modulation for interceptive movements plotted over the original data (grey traces) from Figure 5A. The peak velocity attenuation trend forms an inverted-U shape, and can be split into three zones based on target speed: zone 1 (yellow, 0-10 deg/s), zone 2 (green, 10-40 deg/s), and zone 3 (blue, >40 deg/s).

The inverted-U peak velocity attenuation relationship can be explained by understanding how target speed alters the confidence of the internal model of the moving stimulus. The internal model refers to a subject's predicted trajectory of the moving target, which utilizes: the last sampled position (LSP) of the target, the target velocity, and the neural transmission delay length (EL Keller et al., 1996). It is possible that a higher target velocity could cause the internal model to be unable to update the displacement of that target over the transmission delay, and become more biased by the LSP of the target. We observed this LSP bias in the peak velocity attenuation

trend (Figure 11), which can be split into three zones. In zone 1, when target velocity is less than 10 deg/s, the displacement of the moving target over the transmission delay is minimal, and the internal model is able to update effectively to drive the saccade with very similar dynamics to a stationary target trial. When the target speed is between 10-25 deg/s in zone 2, the displacement of the target over the neural transmission delay is increasing, and the internal model seems to be having a more difficult time updating and driving the saccade with the same velocity as the slower target speeds. The peak of the attenuation trend (middle of zone 2) indicates the transition of the bias in the oculomotor system away from the internal model to the LSP of the target. Lastly, for target velocity greater than 40 deg/s (zone 3), the speed of the target is too high for the internal model to update effectively, so the saccadic system is biased almost exclusively by the LSP of the target, and the interceptive saccade peak velocity again approximately matches that of a stationary saccade. The issue with interceptive saccades in zone 3 is that the saccadic error is extremely high (Figure 9). This theory that the velocity-based internal model becomes less influential to the interceptive saccade programming is supported by the fact that the post-saccadic pursuit gain decreases with target speed, especially for outward moving targets (Figure 10A).

The first to demonstrate an attenuation in peak velocity for interceptive saccades was Keller et al. (1996), but they only tested fast targets (40-60 deg/s) and outward moving targets. Eggert et al. (2005) found that the changes in the peak velocity were distinctly different and showed that saccades to inward moving targets had higher peak velocity compared to amplitude-matched stationary saccades, and saccades to outward moving targets had a lower peak velocity to saccades to stationary targets, although size of the effects were miniscule. They only tested 10 deg/s moving target and only collected a 7-degree movement size. In our data, only monkey BL showed opposite changes for inward and outward moving targets at 15 deg/s across a movement range of 10-20

degrees. Fleuriet et al. (2011) studied saccades where the target movement and the saccade movement were mostly in a perpendicular orientation, and therefore reported the peak velocity for the orthogonal component of the saccade, and found that the peak velocity of the component that corresponded to the direction of the target motion (orthogonal direction) was not different for different movement sizes (8 and 16 deg) and different target movement speeds (7, 14 and 21 deg/s). Unfortunately, these results cannot be directly compared to our results since they did not combine their main sequence for both axes combined, and the target motion and saccade movement vector are in different axes (which is different from what we are collecting).

There were no consistent changes in latency for interceptive saccades compared to the stationary saccade latency (Figure 7). Some animals reacted quicker while others took longer to react and intercept the moving stimulus. Subjects BL and BB waited for the target for inward targets. We tried to limit this by requiring the monkey to make an interceptive saccade within 500ms after the go-cue, but there remains an apparent effect at small movements. Similar to target direction, target speed had little to no effect on latency, and the subjects maintained the trends in latencies across speeds. Fleuriet et al. 2011 reported increased latencies for moving target trials compared to stationary target trials but their results were inconsistent, which closely resemble the inconsistent latency differences noted in this study.

Endpoint error for interceptive saccades was higher than saccade for stationary saccades, which has been reported previously (Fleuriet et al., 2011). Furthermore, the error increased with target speed across all four subjects. The motion direction did play a role in how much error the subject had for an interceptive saccade, as inward moving trials had a lower saccade error compared to the outward moving target. Interestingly, a few subjects showed a positive error for inward moving target, meaning their movement was predictive, or ahead of where the target was

going to be a future target location at saccade end. This predictive error value was negated as target speed increased, presumably because the subjects could no longer track the target as precisely. It is difficult to compare these results to previous studies because most target movements were not radial moving, when the target is moving directly away or towards the fixation position of the subject.

To the best of our knowledge, no previous studies have reported a speed-dependent modulation of peak velocity attenuation between saccades to stationary and moving targets across subjects. This key finding may provide insight into the neural mechanisms that drive the eye movement and help to determine predictions for how position and velocity streams can work in coordination with each other.

Neural Correlates of Interceptive Saccades

The dead interval, approximately 50-100ms prior to saccade onset during which no further information about the environment is taken into consideration, presents an important challenge for interceptive saccade programming (Becker & Jürgens, 1979). This interval causes the subject to predict the path of the target and drive a saccade to a location where the target will be after the dead interval. The main question remains: how does the brain encode a movement to a future location of the moving target? To intercept a moving target accurately, the saccadic pathway needs to compute two components: the last sampled position of the target (position pathway) and the displacement of the target over the dead-interval (integrated-velocity pathway). There are two main hypotheses for the neural correlates to address this challenge: 1) dual-drive hypothesis and 2) streaked activity hypothesis. The dual-drive hypothesis, first proposed by Keller et al. (1996), assumes that the position and integrated-velocity pathways remain separate and add downstream

in the brainstem, specifically in the burst generators, which then project to the motor neurons that enervate the eye muscles. The superior colliculus (SC) resides specifically in the position pathway and that the velocity component is computed in a cerebellar pathway that receives inputs from nuclei that encode both saccade and pursuit related information. In particular, the nucleus reticularis tegmenti pontis (NRTP) and dorsal lateral pontine nucleus (DLPN) have been shown to encode saccades and pursuit. In addition, there has been extensive research on the role and timing of the cerebellar output structure, the caudal fastigial nucleus (cFN), and its contribution to the deceleration of the eyes during a saccade and pursuit. The cerebellum would therefore be tasked with integrating the target velocity over the dead-interval and adding that position to the brainstem burst generators that drive the saccadic eye movements.

Previous analyses on neural control of interceptive saccades focused on spiking activity of individual neurons (Cassanello et al., 2008; Goffart et al., 2017; EL Keller et al., 1996). We have previously proposed that a population level analysis may reveal an alternative to the dual-drive framework Goffart et al. (2017). The so-called streaked activity hypothesis postulates that both position and velocity pathways are integrated together in a central location that drives saccade vector calculation. The SC is a well-studied brain region for saccadic eye movements driven to stationary target, with a retinotopically organized map. Evidence shows that the SC encodes the intended saccade vector through population activity (Anderson et al., 1998; Lee et al., 1988). For stationary saccades, the population activity has been modeled to be approximately Gaussian across the SC distribution, and the saccade vector is thought to be the center or average location, based on the population activity (Anderson et al., 1998; Lee et al., 1988). The neurons in the lower (intermediate) layers of SC have been recorded to be visuomotor, meaning the neurons encode both visual and movement related activity (Munoz & Wurtz, 1995a). The SC, through these

multimodal cells, has the potential to encode the velocity of the moving target prior to the saccade as the visually encoding of the target traverses and “streaks” across the SC retinotopic map. Since the visually-evoked activity will be spread over a different group of neurons, this residual visual energy should modulate the population activity. We anticipate that the population activity would no longer be Gaussian, but rather a streak of activity in the “wake” or previous traversed path of the target in the SC retinotopic map (Goffart et al., 2017). This streak would modulate as a function of target speed and direction, and allow the SC to represent both the position and velocity pathways in order program an accurate interceptive saccade.

Peak velocity for saccades is highly correlated with the vigor of the SC population activity (Smalianchuk, Jagadisan, & Gandhi, 2018). In theory, if the maximum discharge of SC neurons decreases for interceptive saccades, then the peak velocity of the interceptive saccade would also decrease (EL Keller et al., 1996). This explanation accounts for the peak velocity attenuation trend in slow and medium target speed ranges (zone 1 and 2), but does not explain the lack of attenuation at high target speeds (zone 3). As previously mentioned, the saccadic error for these movements is high and the post-saccadic pursuit gain is low for interceptive saccades that catch fast target speeds. This could indicate a change in interception strategy, and cause the animal to expect to make a catch-up saccade to complete the trial correctly, which agrees with previous research (Sophie de Brouwer, Missal, & Lefèvre, 2001). The looming question is whether the SC population activity will reflect that change in strategy and become Gaussian-like, or remain streaked and encode the fast target speeds similarly to slower targets. These experimental results could begin to determine the entry point for cognitive strategies to be incorporated in the saccade programming pathway.

3.0 Superior colliculus population activity analysis for interceptive saccades

3.1 Introduction

When entering a new environment, the visual system naturally scans, making a series of saccades, or rapid eye movements, to shift the gaze on different stimuli. Approximately 80-100 msec before a saccade, no new information about the environment is incorporated into the next saccade due to inherent sensorimotor transduction delays (Becker & Jürgens, 1979). This delay is not an issue for saccades to static stimuli, as the last sampled position of the target is in the identical location at saccade initiation. In contrast, this transduction delay presents a challenge when planning a saccade to a moving stimulus, as the stimulus moves during this time before the saccade. Interestingly, both human and non-human primates can accurately catch moving targets with saccades (Fleuriet et al., 2011; Guan et al., 2005; E Keller & Johnsen, 1990). To accurately catch moving targets with a saccade, subjects must incorporate the last sampled position (position-related information) and the distance the target travels during the transduction delay (velocity-related information). While the neural correlates that underlie saccades to stationary targets have been well studied (Leigh & Zee, 2015), the same cannot be stated for saccades to moving targets or interceptive saccades. Where or how the velocity-related information for a moving target is incorporated into the saccade programming pathway has yet to be elucidated.

To understand the neural basis for interceptive saccades, we focused our efforts on the superior colliculus (SC), a sensorimotor integration hub for the oculomotor system and a necessary structure in the saccade programming pathway (Gandhi & Katnani, 2011). Only two studies have investigated the neural activity in the superior colliculus during the planning and execution of

interceptive saccades (Goffart et al., 2017; EL Keller et al., 1996). The results of each study were based on single-unit recordings of the SC neurons, and they have concluded two different hypotheses: the “dual drive” hypothesis (EL Keller et al., 1996) and the “remapping” hypothesis (Goffart et al., 2017). We will refer to the “remapping” hypothesis as the “streaked activity” hypothesis, as not to confound with previous work in the striate and extrastriate cortex for target remapping (Nakamura & Colby, 2002).

The “dual drive” hypothesis states that the superior colliculus encodes the last sampled position prior to the transduction delay. The displacement of the moving target during the transduction is encoded elsewhere and added downstream in the brainstem (Figure 12A). The “dual drive” was coined from the idea that two separate pathways drive the interceptive saccade for position and velocity to be incorporated into interceptive saccade planning. In contrast to the “dual drive,” the “streaked activity” hypothesis proposed that the SC can encode both position and velocity within its population dynamics. The SC visually encodes the moving target as it traverses across the visual field of the subject. Therefore, the change in position of the moving target is encoded across the population within the SC, and becomes a streak on the SC map. This streak is essentially the visually-evoked activity and leads the movement burst to be streaked as it becomes preparatory activity when the interceptive saccade is programmed and initiated (Figure 12B).

The SC’s population activity for saccades to stationary targets has a roughly Gaussian distribution centered at performed saccade vector location on the SC’s retinotopic map, as previously observed (Anderson et al., 1998). We observed a significant difference in the population activity that programmed interceptive saccades for both inward and outward radial target motion compared to the stationary population activity. Most interestingly, this significant change was streaked along the target’s trajectory, and the streak was scaled as a function of target

speed. These results suggest that the SC is potentially able to encode the interceptive saccade entirely. The non-Gaussian distributed interceptive saccade population activity allows the ability to test how the SC activity encodes the saccade vector. We compared vector averaging and vector summation mechanisms, with the latter showing the most accurate for estimating the observed saccade vector performed.

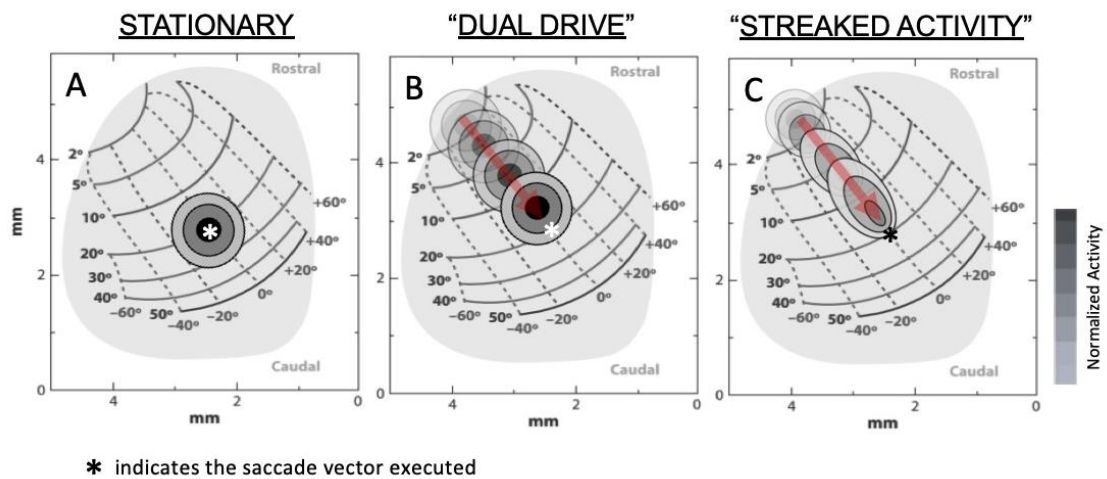


Figure 12: Dual Drive vs. Streaked Activity Hypotheses

Hypothetical movement-related superior colliculus population activity to drive a 20-degree amplitude horizontal movement (average activity +/- 20ms relative to saccade onset) for two different conditions, stationary (A) and moving (B, C). A) For stationary targets, the movement-related population activity in the SC should be a roughly Gaussian mound of activity centered around the performed saccade vector position on the SC map. B) Movement-related population activity for an outward moving target (red arrow is target trajectory) under “dual drive” hypothesis, the population activity has the same Gaussian distribution as seen in the stationary condition (A), but the activity lags the actual movement performed. Take notice of the distance between the peak burst activity (black color) and the performed saccade (asterisk). This difference would be accounted for by another pathway in the oculomotor pathway. C) Movement-related population activity for outward moving target (red arrow is target trajectory) under the “streaked activity” hypothesis, the population activity no longer has a Gaussian distribution, but rather a streak of activity with a trailing edge in the previously traversed portion of the SC map. The peak of the “streaked” population activity is less than in the stationary (A) and the distribution is lagging the performed saccade vector location (asterisk), but the stretch in the activity allows for the lag and decrease in peak burst to be compensated, and therefore the SC can encode the performed saccade vector of the moving target condition

3.2 Methods

General and Surgical Procedures

One adolescent rhesus macaque (*Macaca mulatta*; male, age 10 years) was trained to make saccades to stationary and moving targets. The experimental procedures were conducted on Institutional Animal Care and Use Committee approved protocols at the University of Pittsburgh. Protocols also complied with Public Health Service policy and Human Care and Use of Laboratory Animals guidelines. The animal underwent surgical procedures in an aseptic environment. The subject had a craniotomy fitted with a cylindrical chamber, stereo-tactically positioned and tilted with a 40° posterior angle in the sagittal plane, such that both the left and right SC could be accessed through a craniotomy. The eye movements were measured with a non-invasive infrared eye-tracking system (Eyelink 1000plus, SR Research) and infrared-mirror positioned 45-degrees at the snout of the monkey. Head-restraint was achieved with a custom-fit thermoplastic mask (CIVCO Medical Solutions) (Drucker et al., 2015).

Visual Stimuli and Behavior

An LED-backlit flat-screen television was used to present green squares of 4x4 pixels on a dark gray background and measured to subtend approximately 0.5° of visual angle. Eye position was sampled at 1 kHz for eye tracking. Data acquisition was performed with a real-time LabView-based controller interface (Bryant & Gandhi, 2005). For this study, all animals were trained to direct saccades to stationary or moving targets. Every trial began with presenting a central target, which the animal was required to fixate for 300-500ms. Next, a target appeared in the visual field and either remained stationary or began to move at a constant velocity. The central target remained illuminated for an additional 0-1200 msec (delay period), during which time fixation remained

directed to it. The central target offset cued the animal to make a saccade to the peripheral target within 500ms for stationary targets or 400-700ms for moving targets (see below for justification). A liquid reward was administered if the animal correctly shifted its gaze to the peripheral target and maintained fixation for 100-800ms. If the animal broke fixation by deviating its gaze outside a 3-deg radius around the central target before it was extinguished, or if the animal did not make a saccade in the time allotted, the trial was aborted. In addition to the delay-saccade task, the subject was trained to do a gap task, which is very similar to the delay-saccade task, where the animal is required to begin by fixating on a central fixation point. Directly after fixation, at a randomly assigned time, the fixation point is removed for approximately 100-200ms (gap interval). The animal is required to remain in the window of the central fixation point during this time interval. After the gap interval, the peripheral target is presented, and the subject is allowed to make a saccade to the target, usually within reaction time (approximately 250ms later). The gap trial is essential for stimulation when recording in the SC. It removes any bias in the evoked saccade vector caused by fixation cells being active before stimulation.

For moving target trials, the animal experienced three (low-medium-high) different target speeds (15-30-45°/s) for inward and outward moving targets, and these speeds were randomly interleaved with stationary targets. The moving targets had only horizontal trajectories on the screen, moving inward or outward relative to the fixation target. The starting target position and its speed and direction of motion were randomly chosen but confined along the horizontal axis (see Figure 13B). The initial starting position of the moving target was always the same regardless of target speed (2° amplitude for outward, 26° amplitude for inward moving target), and the target speed determined the delay period used to probe different movement sizes for both inward and outward targets. In addition, the subjects were required to make a saccade within a grace period

(400-700ms after the go-cue) to prevent the moving target from going off-screen (outward) or colliding with the fixation target (inward). In the case of an inward target, the target gets closer to fixation with time. One observed strategy was the willingness to wait for the moving target to come to the subject's initial fixation position. Waiting for the target to reach current fixation could induce only pursuit and not require an interceptive saccade which would not be utilized in this study. The grace period ensured the subject performed the trial correctly and did not wait too long. Saccades were measured with a 30°/s onset/offset criterion. Each saccade was visually inspected, and their onset/offset was manually adjusted as necessary. In addition to the delay-saccade task for moving targets, we also trained the monkey on a "NO-GO" task, where the animal fixated on a central target, and the moving target was presented on the screen, but the central fixation point was never removed. The subject was rewarded if they did not break the central fixation point window for the entire trial. The length of time for the NO-GO trial varied based on the target speed. A slower target required a longer wait time, while a fast target did not require much time. The purpose of the NO-GO trial was to evoke the SC neurons' visual response without the movement-related response.

Neural Recordings and Data Collection

For each recording session, the data was collected using a 24-channel laminar electrode probe (Alpha-Omega, Alpharetta, USA; each contact had ~300 μm diameter, ~1 M Ω impedance, and 100 μm inter-contact distance; see Fig. 13A), and the probe was lowered daily with a hydraulic Microdrive (Morishige, Tokyo, Japan). The probe's trajectory was mainly perpendicular to the SC surface, given the SC chamber placement.

When SC activity was detected, electrical stimulation was applied to individual contacts on the probe (biphasic, 400 Hz, 40 μ A, 200ms) to determine if the probe had reached the intermediate layers of the SC (Massot, Jagadisan, & Gandhi, 2019). After confirming that the probe was positioned in the intermediate layers of the SC with stim-evoked saccades, we collected approximately 150 delay-saccade stationary trials across the contralateral visual field to the SC we are recording. This data will result in a movement-tuning map of the cell. After these movement field tuning trials, we presented approximately ten trials of the gap task. We stimulated 50% of the trials and confirmed each contact's recording location on the SC map. The experiment's remaining trials used the delay-saccade task, randomly interleaving stationary and moving target trials, with moving target direction and speed randomly interleaved as well.

We acquired the neural data by recording on the Scout data acquisition system (Ripple, Salt Lake City, USA). The neural and behavioral data were synchronized at the beginning of each trial through a pulse signal generated from the Scout system. The spiking activity data was acquired with a high pass filter at 250 Hz. Spike times were determined when the recorded signal exceeded a threshold of three times the root mean square of each channel's baseline activity. The neural data was collected from 21 sessions. Recording contacts were only included in the analysis if electrical stimulation of the contact could evoke a saccade, therefore ensuring that all data came from the same layer in the SC (intermediate layer), for a total of 255 contacts of data. The laminar probe contacts can record single neurons, but there is a possibility of two neurons being recorded on the same contact; therefore, our data is generally considered multiunit activity data. Neuron sorting and isolation of single units is not necessary for our analysis because it is included in the same position in the SC.

Data Analysis

Eye movements were analyzed using custom lab software (Matlab), and saccades were assigned onsets and offsets based on a 30°/s velocity threshold criterion. We attempted to emulate a previously attempted approach to estimating 2D population activity in the SC (Anderson et al., 1998). The neural recording data was converted into a continuous signal by convolving the spike trains with a Gaussian function to produce a spike density waveform (Richmond, Optican, Podell, & Spitzer, 1987), and aligned at target onset and saccade onset. We determined the SC map's population activity by combining neural activity from different recording sessions at multiple locations in the SC map. During the experiment, the center of the recorded neuron's movement field was approximated by instructing the subject to make widely distributed points across the display screen and adjusting the target display to locations that yield the most robust response from the neuron. The approximate locus of the neuron's movement was confirmed through stimulation. If the movement field for the recorded neuron was "open" or covered a large portion of visual space, the saccade vector (amplitude and angle) was determined by the saccade end location relative to the initial fixation and used to position the cell in the SC map. Bilateral symmetry exists for the SC, therefore activity from both colliculi can be combined across the left and right hemifields. After determining the best fit rectangular coordinates for the center of the movement field (x,y), we converted the coordinates into SC neural coordinates (u,v) through previously published transformation equations (Ottens et al., 1986):

$$u = B_u * \ln\left(\frac{\sqrt{x^2+y^2+2A+A^2}}{A}\right), \quad (3-1)$$

$$v = B_v * \tan^{-1}\left(\frac{y}{(x + A)}\right) \quad (3-2)$$

The variable u and v refer to the location of the neuron approximately on the rostral-caudal axis and the medial-lateral axis of the SC, respectively in millimeters. The constants will be set to $A=3\text{mm}$, $B_r=1.4\text{mm}$, $B_l=1.8\text{mm}$. After transforming all recordings into SC neural space, we will use a triangularization method for all neural recording locations on the SC map ('griddata' in Matlab, using the cubic interpolation method), which fits the data, smoothing the noise between recorded sites in the map. After we had all the data adequately organized in the SC map and the population activity estimated and smoothed, we wanted to test the potential saccade encoding mechanisms of population average (Lee et al., 1988) and population summation (Goffart et al., 2017; Goossens & van Opstal, 2012).

$$\eta * \sum_i^N FR_i * \vec{V}_i \quad (3-3)$$

Population summation calculation. ' η ' refers to the normalization factor, ' N ', the number of neurons recorded, ' FR ', firing rate of a neuron, ' V ', vector (amplitude and direction) encoded based on location in the SC map.

$$\frac{\sum_i^N FR_i * \vec{V}_i}{\sum_i^N FR_i} \quad (3-4)$$

Population average calculation. ' N ', the number of neurons recorded, ' FR ', firing rate of a neuron, ' V ', vector (amplitude and direction) encoded based on location in the SC map.

To test these theories, we used a time window ± 20 ms relative to saccade onset, averaged each recorded contact's neural activity, and added the neural activity to each equation. The η term in the vector summation equation is thought of as the individual contribution of a neuron to the population activity. When the target is stationary, the η is equation to the sum of all the firing rates, and therefore vector summation and vector averaging give the same estimated saccade vector. We save this η from the stationary vector calculations, and apply the same η to the different moving conditions.

3.3 Results

The difficulty in recording population activity in the superior colliculus is its deep position in the brain, located on the roof of the brainstem, approximately 23mm below the dura, given a 40° posterior sagittal angle. Figure 13A demonstrates the orthogonal trajectory of the multi-contact probe to the surface of the SC and the probe used for recording across the lamina of the SC. Therefore, one way to generate population activity data is by driving a laminar probe to different positions on the SC map and presenting the same stimuli daily (see Figure 13B), creating a pseudo-population. The position of the cells recorded in the SC on a specific recording session was determined through stimulation of each contact (stimulation details in Methods).

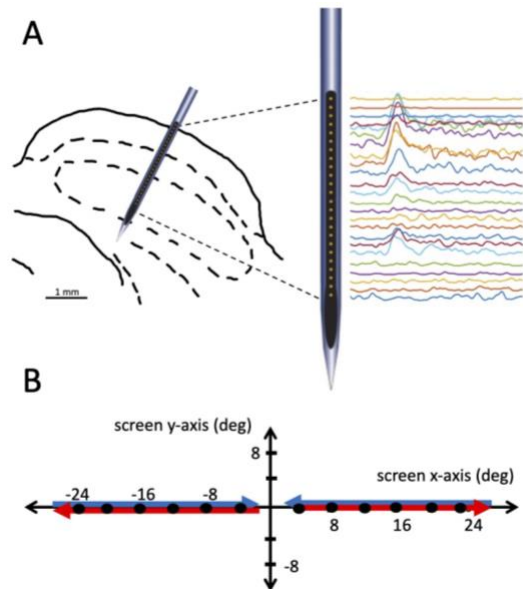


Figure 13: Experimental Setup

A) On the top shows a sagittal-slice schematic of the laminar probe at a 40° from the vertical, and on the right, a snippet of the calculated firing rates of the data collected and analyzed, which has been averaged across several trials of static target data and aligned to target-onset. B) Trajectory of outward targets (red arrow), inward targets (blue arrow), and stationary targets (black dots) presented to the subject for each recording. The starting and ending positions of the moving targets were always the same, regardless of speed; therefore, the delay interval would be adjusted to collect amplitude-matched data for all three speeds collected. The receptive field and movement field for each contact would also be estimated through stationary targets, presented in the quadrant that the neuron seemed most responsive.

For each recording session, the same stationary and moving targets were presented along the horizontal axis (azimuth), and the activity for inward and outward moving targets at three speeds (15, 30, and 45°/s) and three different movement sizes: $7^\circ \pm 2^\circ$, $12^\circ \pm 2^\circ$, $17^\circ \pm 2^\circ$. In Figure 14, the spike density waveform for each contact for stationary (A,D), 30°/s outward targets (B,E), and 30°/s inward targets (C,F). For each trial type, the data was aligned to target onset, saccade onset, and averages in specific windows could be calculated to understand how much activity the neuron has for visual and motor epochs of the trial. One interesting component to this neural recording is that the visual burst onset is delayed for the outward moving target. In panel B, in the left plot, the visual burst seems to occur around 250ms, much later than the visual burst onset at 75ms for stationary targets. This is most likely because these neurons encode a 3.5° amplitude vector and the outward target starts at 2° , so it would take about 50ms for the 30°/s outward target to go from 2° to 3.5° . There are probably different onset dynamics when the target moves across the SC neurons (lagging and slower reaction due to lack of visual burst onset) (Dash et al., 2015).

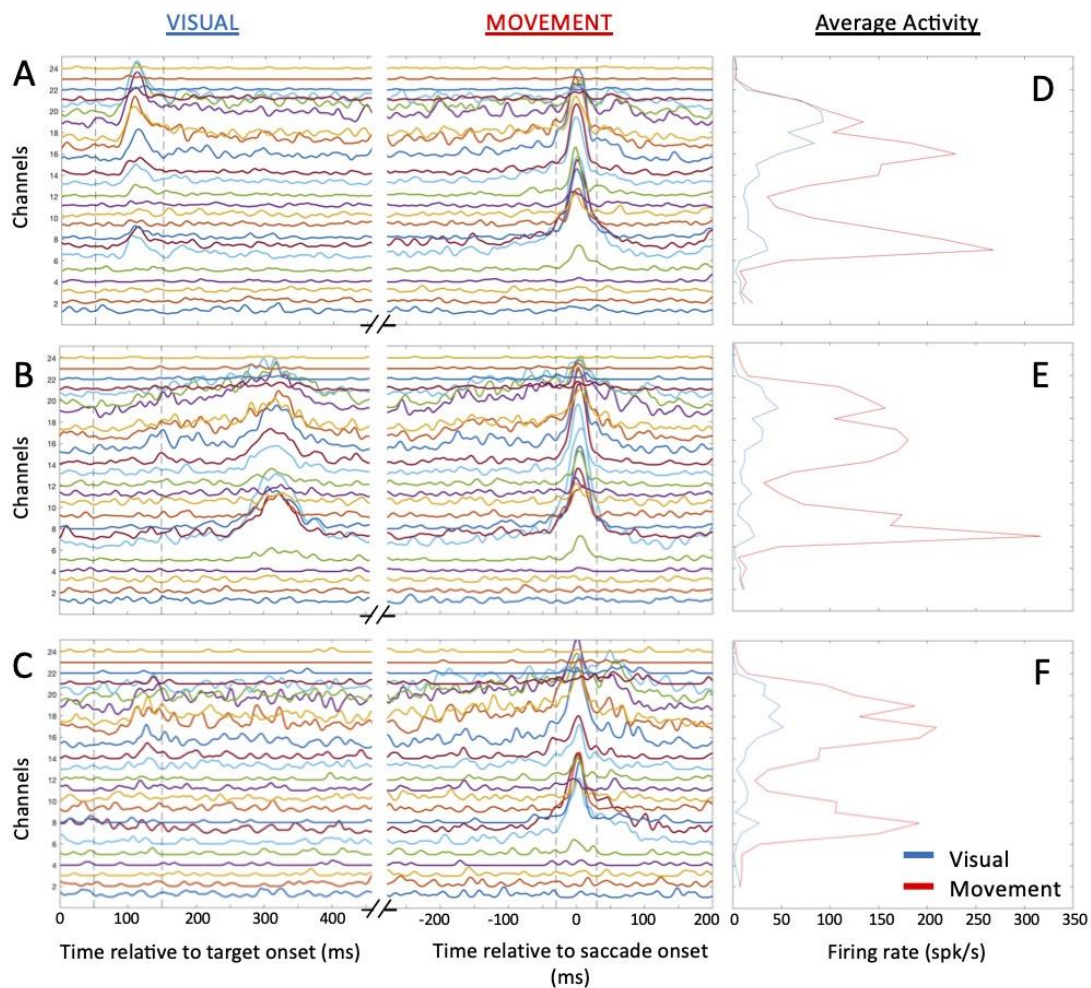


Figure 14: Data Alignment for SC Recordings

Data alignment for SC recordings. This is an example of one session (collected on 3/12/19). All data displayed in this figure is from $7^\circ \pm 2^\circ$ amplitude movements, and the average movement field across all contacts was centered at 3.5° amplitude, 0° angle. The different rows show the different trial types, stationary (top panels), 30 deg/s outward (middle panels), and 30deg/s inward (bottom panels). For panels A,B,&C, the neurons' firing rate on each contact for data aligned to target onset (left plot in each row) and aligned to saccade onset (right plot). For panels D,E,&F, the visual average activity (100ms +/- 50ms from target onset) for the target-aligned data (blue) and the movement average activity (+/- 20ms from saccade onset) for movement-aligned data (red).

As Figure 14 shows data alignment for one of the recording sessions collected for this study. Once the data was aligned, the next challenge was to combine neural activity across sessions. The SC population activity dynamics were visualized after recorded neurons were correctly placed in the SC map according to their preferred vector. Channels with neural recordings were placed with two steps: movement field estimation and stimulation-evoked saccade vector measurement (Figure 15). During the experiment, once we reached the SC activity, we stimulated to ensure we had achieved the SC's intermediate layers, which, when stimulated, will evoke a saccade vector given our stimulation parameters. We then estimated the quadrant that we anticipated the preferred saccade to exist and presented 100-200 trials of stationary delay-saccade trials (Figure 15A). In addition, we stimulated each contact five times each at the end of the recording with a gap task to determine the stimulation evoked vector (Figure 15B). If the two estimates matched, we used these methods as the rectangular coordinates (x,y) for the cell placement. If they disagreed, we looked to the surrounding cells on the recording to distinguish which methods were more accurate. These methods match similar approaches (Anderson et al., 1998).

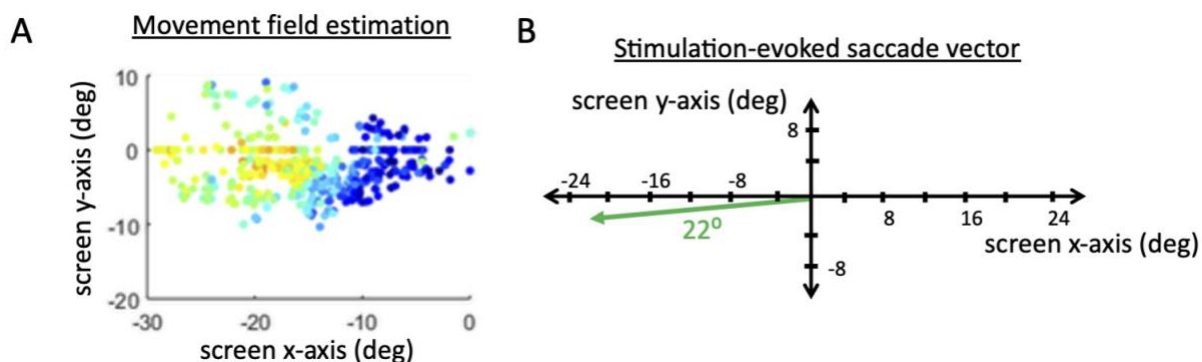


Figure 15: Estimating the Preferred Vector Encoded by the Recorded Neuron

A) One way to estimate the preferred vector is by recording the activity of the neuron during different movements, also known as the movement field. This plot shows the activity of the neuron ± 15 ms relative to saccade onset for the different movements in visual space (denoted as screen access), which are the saccade end locations for each movement. For this neuron, the estimated vector would be 22° amplitude, 190° angle. B) The other way to calculate the preferred vector is to stimulate the contact during the gap task (see methods for stimulation and gap paradigm details). In this example, we measure the stim-evoked vector to be 22° with a 190° angle.

After the cells from all recordings had been assigned a preferred direction in rectangular coordinates, the coordinates were then transformed into polar coordinates (Figure 16A) and then converted from polar coordinates to neural space coordinates in millimeters (Figure 16B) using the Ottes equations (see methods). The data collected from the right or left SC corresponded to the contralateral visual hemifield movements (Figure 16). Since the left and right SC are expected to be symmetrical along the midline ($u=0$ in Figure 16B), we mirrored the left SC cells onto the right SC to produce one SC map. To verify if our cell placement and transformation equation were accurate, we calculated the SC population activity for the three movements that we collected across all 21 sessions: 7° , 12° , and 17° (Figure 17). Previous studies have stated that there should be a gaussian mound of activity centered at the performed movement. Our results would agree to a first-order approximation, as the activity is in the more rostral region of the SC map for the 7°

movements, the middle of the map for 12°, and in the caudal region of the map for 17° movements (Figure 6).

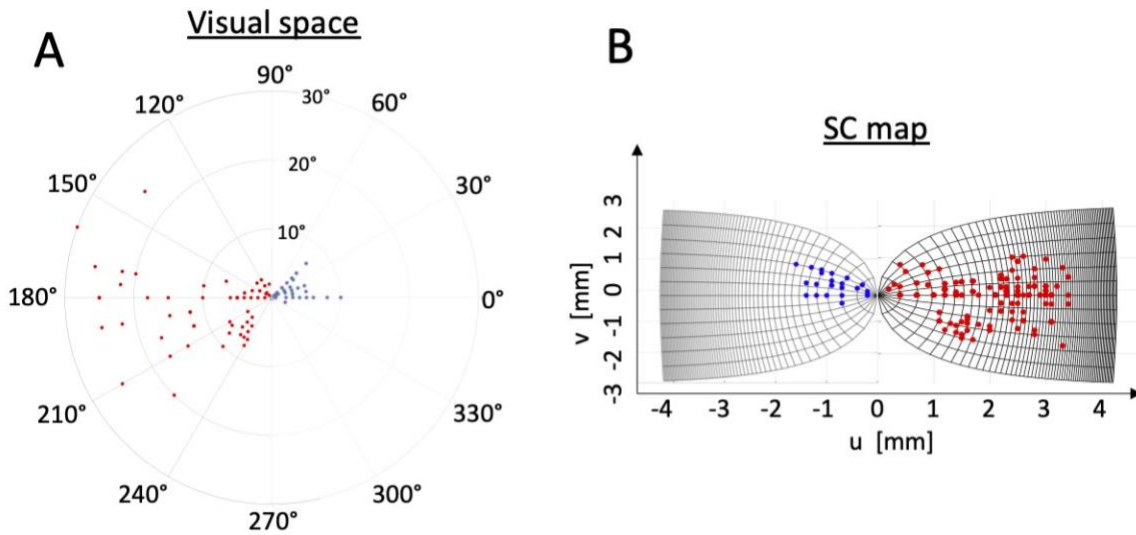


Figure 16: Neuron Distribution and Transformation

A) For each contact, the center of the movement field was estimated and confirmed with stimulation for each contact, and the magnitude (amplitude) and direction (angle) were recorded. This plot displays the 255 contacts we recorded in polar coordinates for the left SC (blue dots) and right SC (red dots). Many contacts have the same encoded position and are therefore overlapped in this plot. B) Through the Ottes equations (see methods), the polar coordinates of the movement fields can be transformed into neural coordinates, u & v (in millimeters).

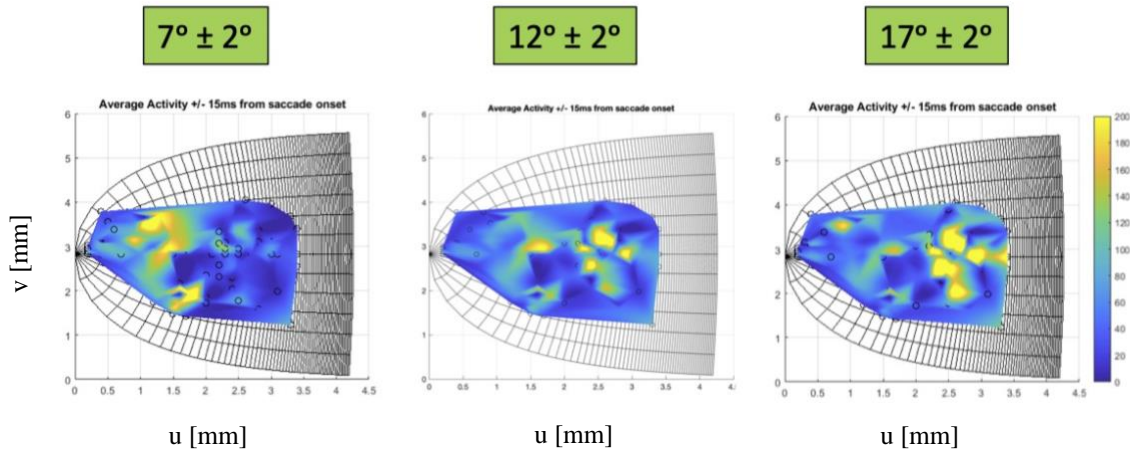


Figure 17: Average SC Population Activity for Different Movement Sizes

Average Population activity for different movement sizes, A) $7^\circ \pm 2^\circ$, B) $12^\circ \pm 2^\circ$, and C) $17^\circ \pm 2^\circ$ in the SC neural space u & v (mm). The data was averaged from a window ± 15 ms relative to saccade onset.

In Figure 18, the SC population activity is computed for stationary and outward moving targets at the three speeds we tested for $12^\circ \pm 2^\circ$. The activity shown is the average activity at the different cell locations ± 20 ms relative to saccade onset. It is difficult to visually compare the population activity between stationary and moving conditions; therefore, we computed and plotted the difference between the static and moving conditions (moving minus stationary). The resulting difference plots are shown in Figure 18 display the SC map areas that are more active for the moving condition (red) and regions of the less active (dark blue) areas than the stationary condition. The key takeaway is that this difference plot shows a spread in the moving condition that is not similar to the stationary condition and does not look symmetrically-distributed nor centered at a slightly lagged SC map position. Also, as outward target speed increased, the intensity of the spread along the target trajectory increased, and the spread laterally to the target trajectory.

Outward Moving Targets

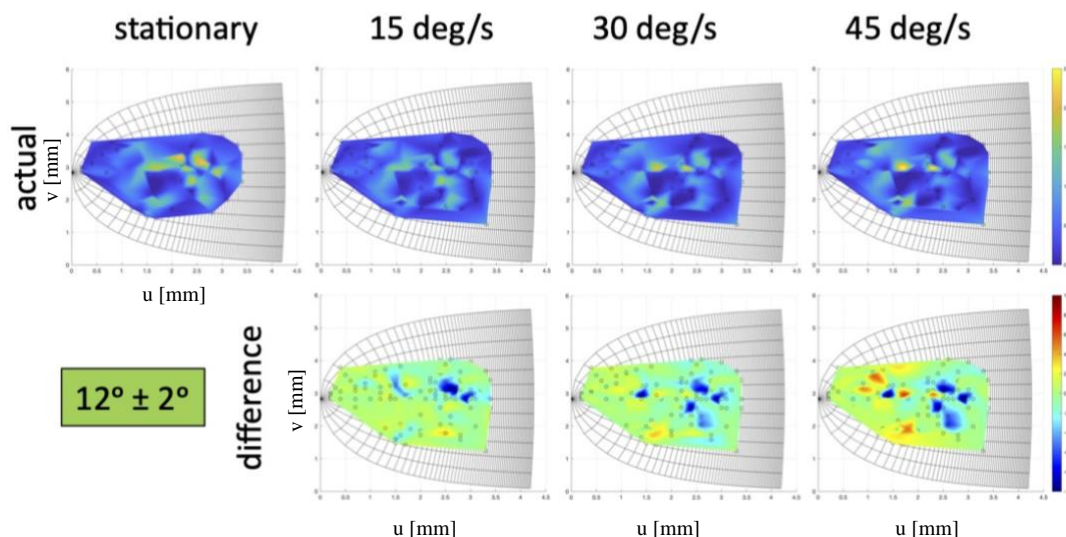


Figure 18: Population Activity in the SC for Stationary and Outward Moving Targets

Population activity in the SC for $12^\circ \pm 2^\circ$ movements for stationary and outward moving targets at three speeds: 15, 30 and $45^\circ/\text{s}$, aligned to saccade onset and averaged over a window ± 20 msec relative to saccade onset. The inward target starts at [2,0] and moves towards [28,0]. The top panel is the recorded activity across the contacts. The bottom is the population activity of the moving conditions with the stationary activity subtracted off. Therefore, areas of the SC map where it's more active for the moving condition are positive (red). The areas where the moving condition is less active will be negative (blue), with the areas where the two activities being equal being indicated by green.

In Figure 19, the SC population activity is computed for stationary and inward moving targets at the three speeds tested for $12^\circ \pm 2^\circ$. Similar to Figure 18, the activity shown in Figure 19 is the average activity at the different cell locations ± 20 ms relative to saccade onset. Again, the difference was compared between the moving and stationary conditions to better compare the inward and static spatial distribution differences. The population activity for inward moving targets is also noticeably different from the stationary distribution. From the difference plots in Figure 19, one can appreciate that as inward target speed increased, the spread along the target trajectory decreased, but the lateral spread relative to the target trajectory increased. Moreover, the overall intensity of the burst profile in the population activity also reduced as inward target speed increased.

Inward Moving Targets

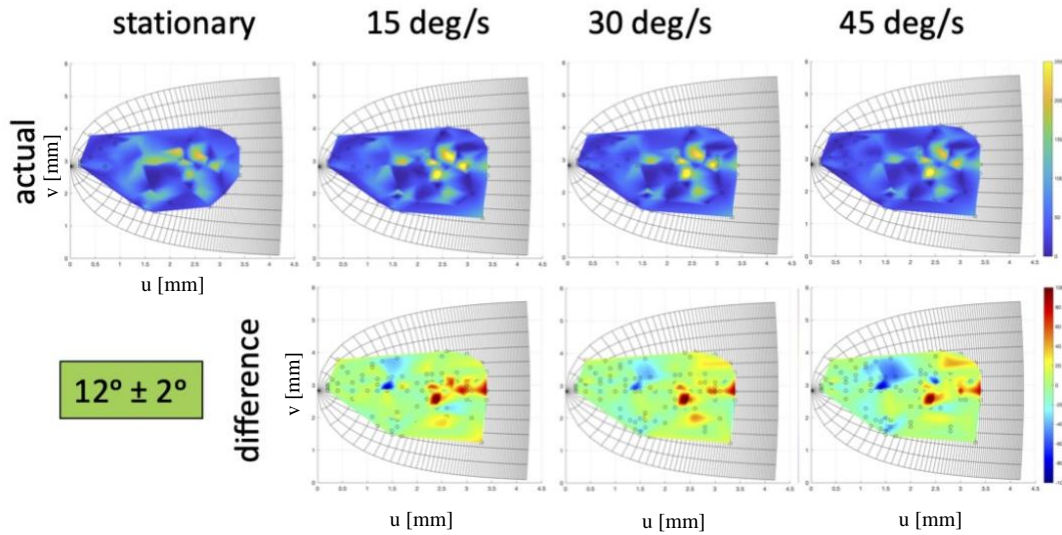


Figure 19: Population Activity in the SC for Stationary and Inward Moving Targets

Population activity in the SC for $12^\circ \pm 2^\circ$ movements for stationary and inward moving targets at three speeds: 15, 30 and 45°/s, aligned to saccade onset and averaged over a window ± 20 msec relative to saccade onset. The inward target starts at [26,0] and moves towards [0,0]. The top row is the recorded activity across the contacts. The bottom row is the population activity of the moving conditions with the stationary activity subtracted off. Therefore, areas of the SC map where it's more active for the moving condition is positive (red) and areas where the moving condition is less active will be negative (blue), with the areas where the two activities being equal being indicated by green shading.

Since the outward target population activity showed a more remarkable change in the intensity and spread, we further investigated the dynamics of the outward target activity in terms of the saccade vector's population activity encodes. We estimated the SC population activity by averaging or summing the activity with a millisecond resolution for $12^\circ \pm 2^\circ$ movements, plotted in Figure 20. The estimated saccade vector for the SC population is calculated for ± 80 ms relative to saccade onset. The top panel of plots is the estimated vector using the average equation (Equation 7, see methods). The estimated saccade vector is roughly stable for the stationary condition and oscillates around the expected vector location. When the target moves outward, the estimated saccade vector is no longer stable and troughs at saccade onset. This trough increased as target speed increased (15°/s: 10.4° ; 30°/s: 10.1° ; 45°/s: 9.9°).

In contrast to the vector averaging method, the vector summation estimated vector peaked at saccade onset (calculated with Equation 6, see methods). The peaks of the moving conditions were less than the peak of the stationary condition, but the peak increased between moving conditions as the outward target speed increased (15°/s: 14.3°; 30°/s: 14.5°; 45°/s: 14.8°). We then took the mean of the vector estimate for each condition ± 20 ms relative to saccade onset (blue-shaded window) and displayed them in Table 2. The mean of the actual movements performed on the trials was also computed to compare and determine which population vector encoding mechanism is better. For all three speed conditions, the vector summation estimate was closer than the vector average estimate.

We wanted to pair our previous behavioral results with our current neural results in addition to testing vector encoding mechanisms. In Table 3, the peak velocity attained for the saccades used to produce the $12^\circ \pm 2^\circ$ population activity is reported. Also, we measured the peak burst achieved by the population activity in the stationary and moving conditions to compare the relationship between peak velocity and peak burst. Based on these results, there is no direct relationship between the peak velocity and the maximum population activity firing rate for interceptive saccades.

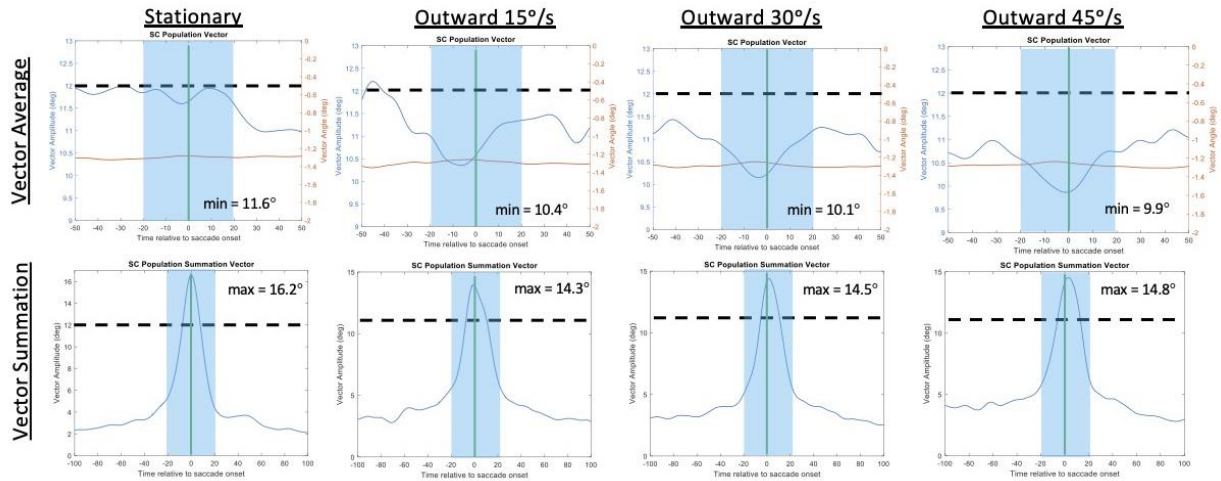


Figure 20: The Timecourse for Saccade Vector Estimation

The estimated saccade vector calculated for stationary and outward moving targets for A) vector averaging and B) summation for all three target speeds (15, 30, and 45°/s). The vector estimate is calculated for each millisecond in the trial ± 80 ms relative to saccade onset. The vector estimates used for comparing to the actual saccade vector were the mean of the estimated vector values over a ± 20 ms window close to saccade onset (light blue shading).

Table 2: Comparison for Vector Averaging and Vector Summation Estimations

	AVERAGE	SUMMATION	Actual
15 deg/s	10.89 °	11.16 °	11.98 \pm 0.46 °
30 deg/s	10.76 °	11.50 °	12.29 \pm 0.45 °
45 deg/s	10.40 °	11.69 °	12.59 \pm 0.36 °

Vector estimates are based on mean population activity ± 20 ms relative to saccade onset.

Table 3: Maximum Eye Velocity and Firing Rate Attained During Stationary and Moving Conditions

	static	15 out	30 out	45 out
Peak velocity (°/s)	832±60	805±109	802±92	833.32±85
Peak Burst (spk/s)	386.75	377.94	419.65	442.28

3.4 Discussion

Several studies have attempted to look at how organisms encode visual information about moving stimuli. For example, the salamander can encode moving target information through a lateral inhibition mechanism in its retina (Leonardo & Meister, 2013). For higher-level organisms with a cortex, specialized brain areas have taken on encoding moving stimuli, such as the middle temporal area (MT) (Newsome, Wurtz, Dürsteler, & Mikami, 1985; Ungerleider et al., 1984). Rapid eye movements have been used to study sensorimotor processes in animals, but most of this research has emphasized stationary targets. Under these circumstances, the metrics and kinematics of saccades have been well characterized (Bahill et al., 1975; Leigh & Zee, 2015), and the neural correlates of movements to static targets are well understood (Anderson et al., 1998; Goossens & van Opstal, 2012; Lee et al., 1988). In contrast, there are currently no studies that characterize the SC's population dynamics for interceptive saccades.

Relationship Between Behavior and Neural Activity for Interceptive Saccades

While the programming and kinematics of saccades to stationary targets has been well studied and understood, only recently have oculomotor scientists started to properly investigate the behavior and neural correlates that underlie interceptive saccades. In the previous chapter, we

investigated the behavioral correlates for interceptive saccades and discovered that target speed is the most consistent driving force behind changes in interceptive saccade behavior, with the key result that interceptive saccades are slowest at medium moving target speeds (10-40 deg/s). Given our behavioral results, we anticipated that there could be changes in the neural activity that would reflect changes in the medium ranges. Unfortunately, the preliminary results shown in this chapter suggest that the SC activity changes more linearly with speed. The only exception to this result is the condition that we did not test a moving target speed slower than 15°/s, and our previous behavioral result had a 10°/s condition. Future testing with a 10°/s target could build more confidence in the neural activity and behavioral outcome. If the SC does not reflect the peak velocity attenuation dynamics, this change may be due to an alternate saccade-related area (i.e. cerebellum or FEF).

Previous Reports of SC Neural Activity for Interceptive Saccades

Therefore, each SC neuron has a movement field or response curve for movements made to a specific region of space. The first neural recordings of interceptive saccades were conducted with single-unit recordings. The effect of a moving target on the SC movement field properties has been preliminary investigated (EL Keller et al., 1996). Keller and colleagues observed a shift in the movement field curve that could be interpreted as a lag in the encoding of the moving target, as the expected saccade vector encoded from this shift would have been to the last sampled position of the target due to the afferent transmission delay (~100ms) (EL Keller et al., 1996). Keller et al. concluded that since the subjects could catch the moving targets, an additional source that incorporates the distance the target travels during the transmission delay would need to be added downstream of the SC to compensate for the lag in the movement fields SC neurons. This deduction was based on the measurement of the maximum discharge rate of the recorded SC

neuron, assuming that the population activity in the SC remains Gaussian for interceptive saccades. This gaussian mound assumption may not necessarily hold when a moving stimulus is the target of the saccade. In addition, Keller et al. only tested outward targets moving at very fast speeds (40-60 deg/s). The study failed to measure how target direction (inward) or slower, and arguably more environmentally relevant, target speeds (0-40 deg/s) affect the SC neuron movement fields. In addition, since they assumed a gaussian-distributed mound across the SC, Keller et al. only reported changes in the movement amplitude for the SC's maximum discharge rate. Still, they did not mention the changes in the movement field edges of the SC neurons. The edges' difference could have provided a clue to the potential for non-Gaussian population activity for interceptive saccades.

Our lab has attempted to fill these knowledge gaps in follow-up experiments to test the Keller conclusion that the SC does not encode any velocity-related information for interceptive saccades. Goffart et al. have captured the movement field for saccades made to both inward and outward moving targets and a wide range of target speeds (10 – 60 deg/s) (Goffart et al., 2017). These results displayed a shift in the SC neuron's maximum firing rate for interceptive saccades that encodes a saccade vector directed to the delayed representation of the moving target (~100ms before saccade onset). While the general observation from Keller et al. remains valid for all neurons recorded, the critical insight from this data is the measurable differences in the edge shifts of the interceptive saccade movement field (Goffart et al., 2017). The inbound movement field edge, or the edge of movement field where the target first enters, for interceptive saccades shifts much greater than the outbound edge of the interceptive saccade movement field relative to the stationary target movement field. These differential changes in the inbound and outbound edges of SC movement fields were present in most recordings. They provided the argument that the SC

population burst activity may not remain Gaussian-distributed for saccades to moving targets. It was this key insight that led us to propose the streaked-activity hypothesis for interceptive saccades.

Intralaminar SC Population Dynamics for Interceptive Saccades

The SC encodes the intended saccade vector to a stationary target through a population response with a burst estimated to be approximately Gaussian distributed across the SC map (Anderson et al., 1998). This Gaussian assumption has been further extrapolated, and the spatiotemporal dynamics of SC population activity for saccades to stationary targets have been well understood (Goossens & van Opstal, 2012). The SC can maintain this position-invariant gaussian mound of activity through intralaminar interactions primarily investigated in the mouse superior colliculus. In general, the SC is made-up of cholinergic excitatory neurons that burst to encode visual and movement-related information at specific points on the retinotopic SC map. There are inhibitory GABA-ergic neurons that surround each excitatory neuron. The inhibitory neurons receive inputs from the excitatory neurons and inhibit the neighboring excitatory. Therefore, when an excitatory burst, a local excitation burst, and a surrounding, or global, inhibition to cells nearby. We will refer to these intralaminar connections as a local-excitation-global-inhibition (LEGI) network.

LEGI networks are specialized for creating a locus of activity and dampening a system (Meredith & Ramoa, 1998; Phongphanphane et al., 2014). This intrinsic mechanism is a critical feature to the SC to prevent noise from disrupting the intended saccade programming. If an input pulse were applied to a single point in the map, there would be a ripple type effect in the map, similar to a pebble dropping into a pool of water. The rebound of the water to the pebble falling through the water surface is a similar dynamic to the SC's population activity for a stationary target. In the case of a moving stimulus, instead of a single pebble, a series of pebbles are being

dropped into the pool along the trajectory of the moving target and at the frequency of target position updating in the oculomotor system. After the first pebble is dropped, every subsequent pebble has a diminished water rebound. The last pebble evokes an inhibitory effect on the position where the next pebble will hit the water. If the speed of the hand dropping the pebbles is increased, as it drops pebbles, the pebbles will drop with an increased velocity and cause a more significant ripple in the pool of water. We noticed this dynamic in our results, in Figures 18 & 19, and in Table 3, the spread and the intensity of the population activity increased as target speed increased. This pebble-water example is an excellent metaphor to emphasize the spatiotemporal dynamics that can lead to a streak of activity along the target’s path and how that streak can change as a function of target speed.

The Neural Basis of Interceptive Saccades

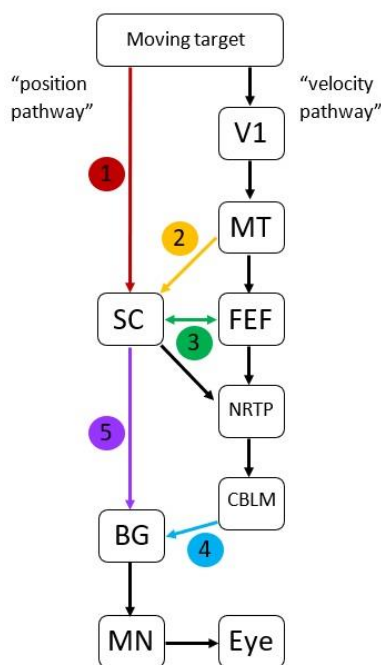


Figure 21: Proposed Oculomotor Circuitry that Plans and Executes the Interceptive Saccade.

The two main pathways that need to be tracked for intercepting a moving stimulus are the target’s position and velocity. The prevailing viewpoint currently separates those two streams of information shown in Figure 21 (Robinson, 1973). When a target is stationary, the visual and movement-related information can all be accounted for in the superior colliculus (SC), as numerous studies have determined that the SC has both visual encoding of the target position as well as movement encoding for the performed saccade vector, and is, therefore, the pathway to the SC (**path1**) is thought to be the position pathway (Gandhi & Katnani, 2011; EL Keller et al., 1996). Alternatively, the primary visual cortex (V1) is believed to be in the “velocity pathway”

since it projects to the middle temporal area (MT), which has neurons that visual receptive fields and discharge for moving stimuli with specific directional tuning and increase in firing rate with speed of the targets (Newsome et al., 1985). A few studies have demonstrated direct projections from MT to SC (path 2), but there is no evidence regarding the information relayed in these MT-SC connections (Newsome et al., 1985; Wall et al., 1982). Therefore, there remains the possibility for SC to receive velocity-related information, but evidence needs to be provided to support this hypothesis. MT project information to the frontal eye fields (FEF) (Cassanello et al., 2008). FEF is a brain structure with stationary saccade activity (similar to SC) and sends and received information to/from SC (path 3). There is evidence that FEF shows direction sensitivity and gain modulations for different speeds during interceptive saccade (Cassanello et al., 2008) but how this information is incorporated downstream is unknown. Potentially FEF sends this information to SC; therefore, the SC remains a possibility for integrating FEF velocity information. Both SC and FEF output to the nucleus reticularis tegmenti pontis (NRTP) which is an input structure to the cerebellum (CBLM) and shows bursting dynamics for saccades to stationary targets (Mustari, Fuchs, & Wallman, 1988; T Raphan & Cohen, 1978; Thier, Koehler, & Buettner, 1988). CLBM may integrate the velocity-related information to correct the position pathway signal from the SC and adds this downstream (path 4) to the burst generators (BG) (Gandhi & Katnani, 2011; Katnani & Gandhi, 2012). While this remains a possibility, it is easier to rule out the previously mentioned pathways before diving into the CBLM circuitry, arguably the most complex network in the brain. Therefore, the movement burst generated as a population activity in the SC will be recorded (path 5) to determine if the SC has access to the velocity-related information based on modulations' activity in normal and inactivated states (Gandhi & Katnani, 2011).

Limitations and Future Directions

There are several limitations of this work, the most critical limitation being the quantity of data included and the use of only one subject. More data has been collected for this subject and will need to be included to build more confidence in the population activity calculated. One assumption that we made when plotting the population activity is the symmetry between the upper and lower visual hemifields in the SC map (v-axis). Recent work has shown that this is mostly not the case (Hafed & Chen, 2016). More of the SC map is devoted to the upper visual hemifield over the lower visual hemifield. Adjusting the map could change the upward, downward, and oblique population activity. Since we focused our study on horizontal saccades, modifying our maps should not significantly alter our population activity results and saccade vector estimates.

In the results shown in this chapter, the time bin of ± 20 ms relative to saccade onset was utilized consistently. While this time bin is generally accepted as a window in which SC activity will play a role in driving and planning the saccade performed, more recent research has been published that supports that the SC influences the movement, not only at the beginning of the movement, but rather throughout the entirety of the saccade, with a delay of ~ 7 ms (Smalianchuk et al., 2018). In addition, we have developed videos of the population dynamics, and there seems to be a wave-like activity in the moving conditions. Therefore, a more careful temporal analysis needs to be completed to investigate a potentially significant population dynamic for interceptive saccades. While this study is elucidating the SC activity for interceptive saccades and proposing that the SC could intrinsically encode and drive an accurate interceptive saccade, we acknowledge the alternate brain regions that most likely also contribute to programming and executing interceptive saccades, such as the frontal eye fields (FEFs) and the saccade-related portions of the cerebellum (i.e., caudal fastigial nucleus).

In conclusion, this chapter's preliminary evidence supports the idea that the SC activity is influenced by the moving target and changes when generating a saccade to a moving stimulus. The changes in the population activity can be modulated with moving target speed. To our knowledge, this is the first study that has investigated the spatiotemporal dynamics of population activity in the SC for interceptive saccades. This study has demonstrated the usefulness of using interceptive saccades as a tool to analyze saccade vector encoding across the SC population activity.

4.0 Neural Network Model of the Superior Colliculus

Computational modeling can be an effective tool in testing potential mechanisms. In this study, we are interested in the saccade vector encoding mechanism of the SC population activity for interceptive saccades. A few computational models of the SC have attempted to answer how the SC fits into the oculomotor pathway for saccades to stationary targets (Kasap & van Opstal, 2017; Optican & Quaia, 2002). We intended to utilize previously developed models and optimize them to simulate SC activity during saccades to moving targets.

4.1 Methods

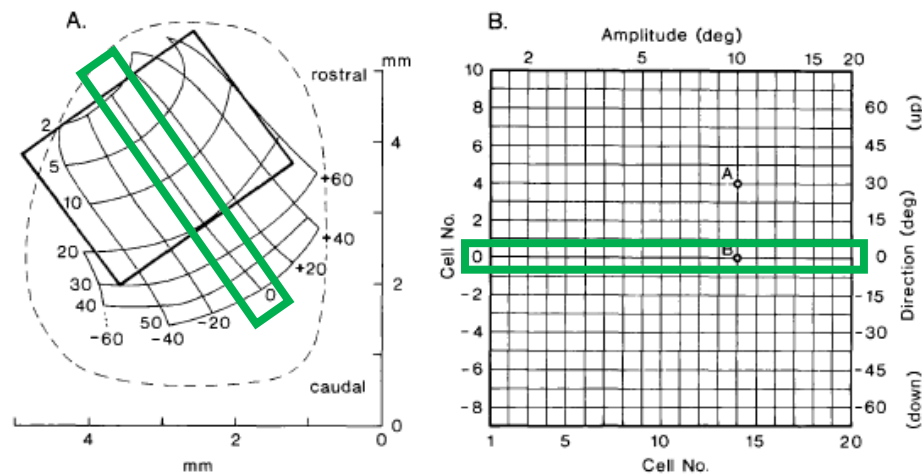
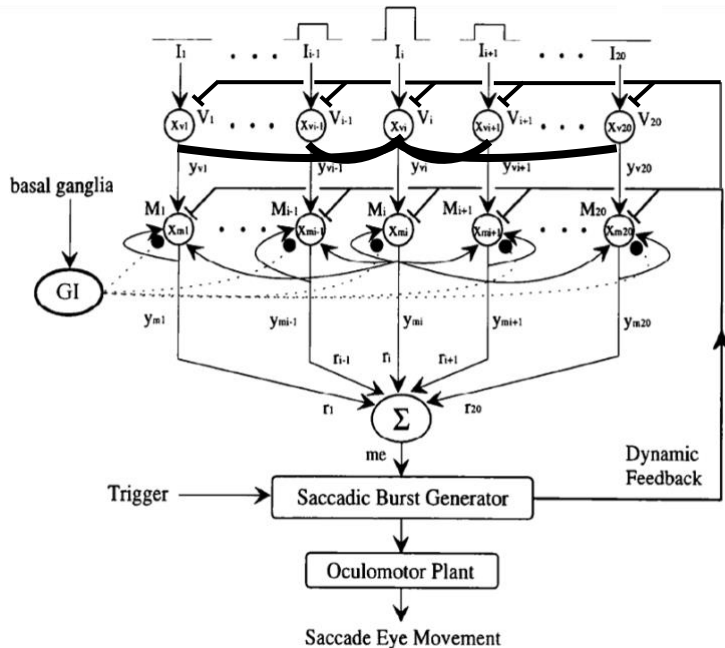


Figure 22: The Model Transformation of the SC

A) Schematic showing an intralaminar cross-section of the SC and its retinotopic spatial mapping. B) The grid of nodes used to represent the SC in the model, with the SC rostral-caudal axis (amplitude) described in the x-axis nodes and the SC medial-lateral axis (angle) defined in the y-axis nodes. Note that the green rectangle in both represents the same subspace, where activity in this region would indicate purely horizontal movements.

We adapted a previously published model (Arai & Keller, 2005). The model encompasses the entire oculomotor pathway: the input to the model is a visual target position. The output of the model is the expected gaze shift (see Figure 23). We chose this model because it also provides the ability to model a neural network model of the SC and observe the population activity in the SC's visual and motor layers. The model simplifies the SC into two layers (visual and motor), with each layer being described by a grid of 20 x 20 coupled first-order equations, modeling the retinotopic SC map in rectangular coordinates (Figure 22B), and each node represents an ensemble of SC neurons with similar tuning responses. This model allows for intralaminar and interlaminar weights to be specified, and Figure 23 shows a schematic of the intrinsic connections within each layer and across the two layers. The neural network equations and the variables utilized are explained below.



Schematic of the modified Arai model for one row of the rostral-caudal axis in the SC model, shown as the green outlined area in Figure 6. The model has two main SC node layers (X_v & X_m), where the 'ith' node refers to the proximity to the node being computed. Arrows indicate positive input, while the stump-end projections indicate negative input to the cell nodes.

Figure 23: Schematic of the Modified 1D Arai SC Model

(4-1)

Visual neuron pool (V)

$$\tau_v \frac{dx_{vi}}{dt} = -x_{vi} + g \frac{dl_i(t - \Delta t)}{dt} + \sum_j w_{vij} Y_{vj} - wvf_i * FB \quad y_{vi} = f_v(x_{vi}).$$

(4-2)

Visuomotor neuron pool (M)

$$\tau_m \frac{dx_{mi}}{dt} = -x_{mi} + \sum_j w_{ij}(\lambda) y_{mj} + w_{i_i} y_{vi} - wvf_i * FB \quad y_{mi} = f_m(x_{mi}).$$

The visual location of the target is converted into an input current for the model ($dl_i(t)/dt$), which has a delay (Δt) of 60 ms to account for the afferent transmission delay in the visual system. This activity provides input to the superficial visual layer node (x_{vi}). The activity of each node in the visual layer (x_{vi}) is determined by the visual input, the time constant (τ_v), the output activity of neighboring visual nodes (y_{vj}), which has a weight (w_{vij}) associated with the proximity. The weight function associated with proximity to the node of interest is shown in Figure 22A. Each intermediate motoric layer node (x_{mi}) activity has a time constant (τ_m) that encodes the response dynamics for the activity. The cell nodes are driven by the output of the visual nodes and its weight function (w_{vij}), neighboring node output (y_{mj}) with the weight function (w_{ij}) determined by the function seen in Figure 8B. Once a movement begins, there is feedback from the burst generators in the brainstem that provides inhibition to reset the oculomotor system to encode the new retinotopic positions of targets that the next movement can begin to be encoded by the model. The output function of each layer (Y_v and Y_m) is a non-linear process. ‘GI’ is global inhibition from the basal ganglia (Hikosaka, Takikawa, & Kawagoe, 2000) and is present in the visuomotor layer equation as lambda, which has the equation $w_{omij}/(1+GI)$, where interconnection weight, w_{omij} , is a

constant value. GI inhibits activity to spread through intralaminar connections until the signal to generate a saccade is initiated and the GI signal goes to zero.

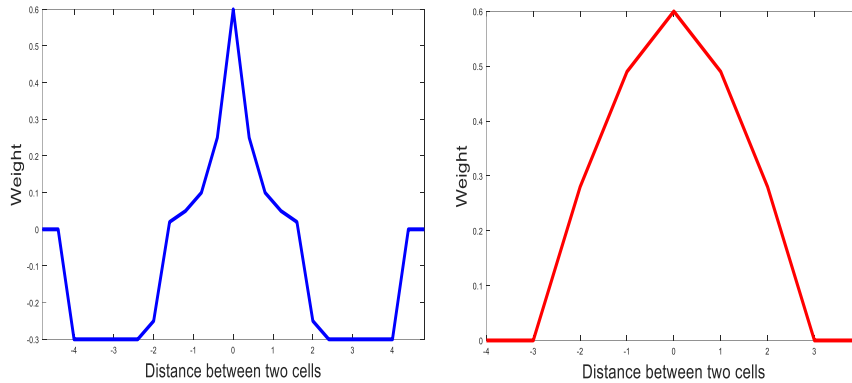


Figure 24: Intralaminar Weights of SC Layers

Intralaminar weight distributions for the superficial (A) and intermediate (B) layers. These distributions are supported by previous research that determined the relative excitatory-inhibitory balance in the layers of the SC (Phongphanphane et al., 2014).

4.2 Results

The results of our SC simulations are shown in Figure 25. The column A of Figure 25 shows the stationary activity for a 10-degree horizontal target, which we fit the model to have a symmetrical-mound of activity centered at the target location at the time of saccade onset (dashed white line at 300ms), and therefore future saccade vector location. We then presented outward and inward targets (Fig. 25, column B & C) and the activity at saccade onset is no longer symmetrical, but rather streaked in the previously traversed location in the SC map. The main goal of the model is to be able to test whether the trained neural network model can physiologically relevant inter- and intralaminar weights. We anticipate that the model will determine whether a population summation or population average calculation is appropriate for driving saccadic eye movements.

It will be interesting to observe the trained weights between nodes for the intralaminar weights to mimic the expected weights we have been using (Figure 8) and the trained burst generator weights that incorporate the summation or average.

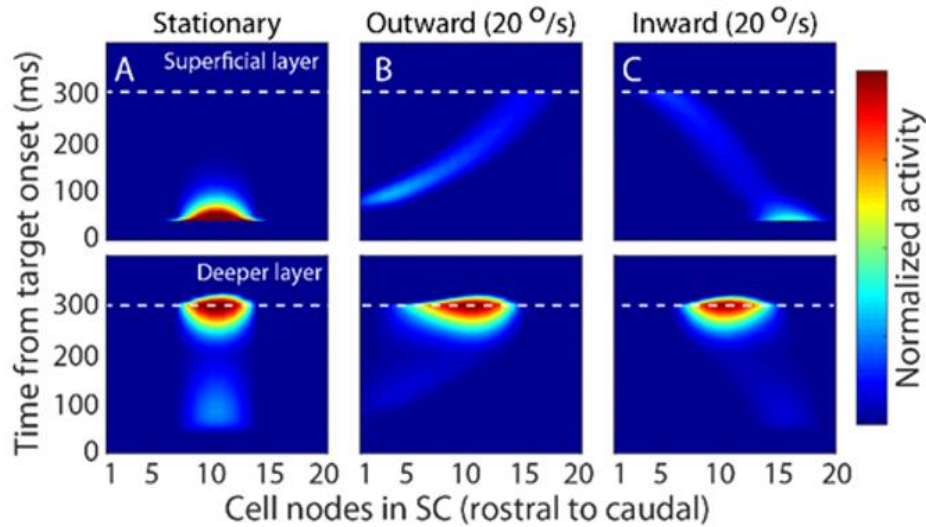


Figure 25: Stationary and Moving Target Simulations of 1D SC model

SC model simulations for A) a stationary case, B) a 20 deg/s outward moving case, and C) a 20 deg/s inward moving case. The top panels are the superficial layer output, and the bottom panels are the deep, motoric layer activity. At 200 ms, the global inhibition is removed, allowing activity to build in the motoric layers. The saccade onset (dashed lines) occurs at 300 ms, following which inhibitory feedback diminished the SC bursts in both layers.

4.3 Discussion

As mentioned in the previous chapter, recent work discovered that the SC map might not be symmetrical across the horizontal azimuth. There may be more representation of the upper visual hemifield in the SC (Hafed & Chen, 2016). This may be a possible explanation if our trained

neural network does not work with the current symmetrical layout we have described above. We remain open to the possibility of adjusting the SC mapping to account for this observation. Another potential adaptation to the model is direct visual input to the motoric layers. We know the visual burst of visuomotor neurons in the intermediate layer can be simultaneous with the visual burst in the superficial layers (Gandhi & Katnani, 2011). This adaptation may not change the model's output, but the visuomotor neurons' temporal activation will be more tightly coupled with the trained neural data.

The successful simulation of the completed model will provide our research with a tool to probe both spatial and temporal dynamics in the SC for interceptive saccades that we currently cannot observe. An overarching goal of this model would be to produce saccades to moving targets and mimic smooth pursuit after the saccade that is executed by the subjects during the trials. Adding the ability to study both saccades and pursuits within the same system has been investigated from the aspect of catch-up saccades when saccades are executed when smooth pursuit falls behind the moving target (Blohm, Missal, & Lefèvre, 2003; S. de Brouwer et al., 2002; Sophie de Brouwer et al., 2001).

Future Direction

Similar to the Arai model, in the future we will implement a gradient-descent learning algorithm in two phases: In phase 1, we will train the model with stationary targets and moving targets and compare the population activity in the model to the actual estimated activity in Chapter 3 to determine if the model is accurately capturing SC spatiotemporal dynamics. In phase 2 of training, use the SC population data to train the burst generators' weights. We have a general physiological estimation of these weights given previous results (Phongphanphanee et al., 2014),

so our initial conditions may start with these physiologically relevant parameters to guide the model to find weight parameters expected in the subjects.

5.0 Conclusions and Future Directions

5.1 Conclusions

In summary, we investigated the behavior and neural correlates of interceptive saccades. The main finding was that target speed plays a critical role in modulating behavior and SC neural activity. Regarding behavior, most of the saccade metrics that we investigated seemed to be more idiosyncratic than previously reported. The only consistent effect was a decrease in peak velocity for interceptive saccades compared to amplitude-matched stationary saccades. We determined that there was an inverted U-shaped relationship between peak velocity attenuation and target speed. Therefore, when subjects intercepted a target with a medium speed (10 - 40°/s), they showed significant peak velocity attenuation. We also investigated the SC population activity for interceptive saccades and discovered a streak of activity that spreads more and increases in bursting intensity as target speed increased. The preliminary results demonstrate that ‘vector summation’ may be the better saccade encoding mechanism over ‘vector averaging’ for the SC population activity. Finally, we have developed a computational model of the SC to be able to predict neural activity modulations with different target speeds (5 to 60°/s), directions (inward, outward), and trajectories (vertical, horizontal, oblique). We can also use the model as a tool to: inactivate portions of the SC (mimicking inactivation experiments), change the input timing to reflect better the information flow of moving target position and velocity, or test different saccade encoding mechanisms. There are still many questions regarding the SC’s role in the interceptive saccade’s programming and execution. Nevertheless, we can definitively say that the SC activity reflects changes due to target speed, demonstrating that the SC encodes both position and velocity.

5.2 Future Directions

Future Analyses with Current Data

While we were able to accomplish the goal of observing population activity for interceptive saccades, several analyses were out of the scope of this dissertation. Still, they would be exciting and potentially insightful to investigate. Below is the list of investigations that would be the next steps for this understanding SC involvement in interceptive saccades:

- 1) Dynamics of interceptive saccades
- 2) Incorporating neural recordings into the computational model
- 3) Testing the landing time hypothesis for interceptive saccades
- 4) LFP analysis for interceptive saccades
- 5) Temporal stability of interceptive saccade data
- 6) Machine learning analysis for interceptive saccade data

1) In Chapter 2, we investigated the saccade metrics of interceptive saccades: peak velocity, duration, latency, and saccade error. But there are several key factors to these movements that could be further investigated, such as the kinematics of interceptive saccades, which includes: acceleration, deceleration, onset-to-peak, peak-to-offset. These are essentially already analyzed and could hold more essential aspects of the interceptive saccade behavior to help us pair with the neural data and draw correlations for how eye movements are generated and what role the SC plays.

2) The computational model is not an exact copy of the model that Arai et al. generated (Arai & Keller, 2005). The output of our model is just the 2D population activity of the motor layer in the SC. Arai et al. attached an eye plant to their model, so their final output was eye displacement during the saccade. This is a future direction with our model, to add the eye plant and translate the SC population data into eye movement data. Once the eye plant is added, we can train the neural network on the SC recordings with both stationary and moving targets and test the vector averaging and vector summation mechanisms. This model would help verify our findings from Chapter 3 and add evidence to support our results.

3) There is a proposed idea that the SC activity is most reflective by the landing time, which is the time from the 'go cue' in the trial to time of saccade offset (Bourrelly, Quinet, & Goffart, 2015; Goffart, Bourrelly, & Quinton, 2018; Quinet & Goffart, 2015). The data collected during our neural experiments (Chapter 3) had a control for this hypothesis, as we had different starting positions for the different target speeds and had no delay (step trials) for interceptive saccades, therefore making their landing time essentially the same (aside from random differences in latency). This step-trial data could be analyzed and compared with the delay-saccade data to see if the delay affects the SC activity and the saccade encoding vector estimation. It's possible that the role of the SC could change if there is less of a delay between target onset and go-cue.

4) In Chapter 3, we analyzed the spiking data for SC neurons, but we also collected the local field potentials (LFPs) during our experiments. Generally, the spiking data is thought of as the neuron's output, and the LFPs are considered the input to the neurons (Massot et al., 2019). Therefore, we propose that if the SC receives additional inputs for the interceptive saccade due to the moving target, then the LFPs for interceptive saccades could be significantly different from the stationary saccade LFPs. It is currently unknown whether the SC intrinsically encodes the moving

stimulus based on changes in position or that the SC receives input from velocity-encoding areas (i.e., frontal eye fields or area MT). The data is already collected, it just needs to be analyzed. The issue is that we have a very vague understanding of the LFP in the SC's stationary condition, so as more research is published for LFPs in the SC, we will be better able to analyze the differences in the LFPs for the interceptive saccade.

5) The SC neurons are considered visuomotor due to the neurons' ability to burst for the visual presentation of a stimulus in their receptive field and burst for a saccade planned into their movement field. A previous member of our lab, Dr. Uday Jagadisan, investigated this multiplexing property to understand why the neurons don't drive an eye movement with the visual burst (Hall & Moschovakis, 2003). Dr. Jagadisan discovered the main reason is that the SC neurons are uncoordinated with other SC neurons during the visual epoch (low stability) but highly coordinated leading up to and during the saccade onset (high stability) (Jagadisan & Gandhi, 2019). It would be interesting to use this stability analysis with the moving target data to see how unstable SC neuron activity is leading up to the interceptive saccade and determine if the stability for an interceptive saccade is maintained for comparable durations to the stationary saccade activity in the SC.

6) Our lab is also investigating the visual-to-motor transformation of moving target data regarding machine learning algorithms, which look at the variability in multiple dimensions of the recorded data. The concept behind this analysis is that the SC data will live in a visual subspace during the target onset and then transition to a movement subspace leading up to and during the saccadic movement, similar to the optimal subspace hypothesis investigated for arm movements in motor cortex (Batista, 2020; Churchland, Byron, Ryu, Santhanam, & Shenoy, 2006). Our initial analyses in the lab have demonstrated the separability between the visual and movement time

points during the delay saccade trials for stationary targets. It would be fascinating to compare the change in the interceptive saccade data dynamics to the static target data.

Future Experiments

- 7) FEF inactivation experiments
- 8) MT experiments – inactivation and optogenetics
- 9) Investigate the role of the cerebellum for interceptive saccades

7) Based on our results in Chapter 3, the next step in the research would be to identify if the SC activity changes due to target speed are intrinsic or external. One way to investigate this would be to inactivate structures that encode moving targets' velocity and have projections to the SC. Two main structures that would be ideal inactivation targets would be FEFs and MT. The frontal eye field (FEFs) region in the frontal lobe cortex also has saccadic bursts and can generate eye movements when stimulated (Robert H. Wurtz et al., 2001). Cassanello et al. showed that FEFs encode velocity-related information for interceptive saccades and that these neurons could potentially encode the prediction for saccades to moving targets (Cassanello et al., 2008). Specifically, they provided evidence of changes in the gain of the FEF neurons that changes with the target speed. While the results from Cassanello et al. are interesting, how information regarding FEFs is fed into the saccade pathway has not been thoroughly proposed. Also, there is little evidence supporting FEFs to pontine structures directly (Segraves, 1992). FEFs are known to project strongly to the SC, and therefore the SC should display any information the FEFs is encoding if it is relevant to the interceptive saccade (Hanes & Wurtz, 2001). Inactivating FEFs

during interceptive saccades with muscimol might reveal a significant change in population activity which could help build our understanding of how the SC and FEF communicate.

8) The middle temporal area (MT) has sharp tuning for direction and broadly encodes changes in the speed of moving stimuli (Raiguel, Van Hulle, Xiao, Marcar, & Orban, 1995). Previous studies have shown that MT contributes to interceptive saccades' accuracy, as subjects fell short of the moving target when MT was inactivated with muscimol (Newsome et al., 1985). It is known that MT directly projects to the SC and that these projections have been observed to project in a topographic manner (Ungerleider et al., 1984; Wall et al., 1982). The unknown remains what information is transferred from MT to SC and how it influences SC population activity. To investigate the effect the direct projections from MT have on the SC, we could inactivate the terminals of MT that project to SC. Using optogenetic stimulation to inactivate infected terminals in the SC, we can observe how the SC population activity changes when generating a saccade to a moving target without the information from the direct projections. This selective inactivation allows all other MT connections to remain unaffected by optogenetic stimulation and should be a good test of whether the direct projections impact the SC population activity. The optogenetic inactivation experiment could use a red-shifted cruxhalorhodopsin (Jaws), a highly light-sensitive chloride pump that will inactivate the infected neurons. Jaws has been demonstrated to have three times the photocurrents as other inhibitory opsins (Chuong et al., 2014). Also, red light traverses through tissue best since it is a low-frequency light, capturing a larger volume of tissue.

9) The caudal fastigial nucleus (cFN) is the output nuclei of the cerebellum. Direct projections have been identified from the cFN to excitatory burst neurons (EBNs) and inhibitory burst neurons (IBNs) in the peripontine reticular formation (PPRF), providing anatomical evidence to support the hypothesis that cFN output could add downstream from the SC in the brain stem

(Scudder, 2002). The primary input to the cFN is the oculomotor vermis, which receives target velocity information from middle temporal (MT) and medial superior temporal (MST) areas in the cortex indirectly through the dorsal-lateral pontine nucleus (DLPN) and nucleus reticularis tegmenti pontis (NRTP) (Dicke, Barash, Ilg, & Thier, 2004; Ungerleider et al., 1984). The velocity-related motor activity has been observed in cFN for smooth pursuit, and this activity has been determined to be essential for consistent pursuit-related movements (Fuchs, Robinson, & Straube, 1993; Straube, Fuchs, Usher, & Robinson, 1997). Stationary target studies have identified cFN output to encode saccade metrics, specifically saccade acceleration and deceleration (Dean, 1995; Fuchs et al., 1993). The underlying concept of cFN output is to assist in the accuracy of saccades (Goffart & Pélisson, 1998). As previously mentioned, saccades to outward moving targets have a more prolonged deceleration phase, while saccades to inward moving targets have a shorter deceleration phase (Guan et al., 2005). This modulation to the saccade could be due to a change in the gain and timing onset of the cFN output. Therefore, the activity of the cFN will be collected in both saccades to stationary and moving targets. The differences in the firing rates and timing of the bursts will determine the mechanistic changes in the cFN during interceptive saccades. We would expect the fastigial neural firing pattern to correlate with target velocity and modify the saccade program to complement the SC's programming information, such that the interceptive saccade is accurate.

Bibliography

- Anderson, R. W., Keller, E. L., Gandhi, N. J., & Das, S. (1998). Two-dimensional saccade-related population activity in superior colliculus in monkey. *Journal of neurophysiology*, *80*(2), 798-817.
- Arai, K., & Keller, E. L. (2005). A model of the saccade-generating system that accounts for trajectory variations produced by competing visual stimuli. *Biological Cybernetics*, *92*(1), 21-37. doi:10.1007/s00422-004-0526-y
- Bahill, A. T., Clark, M. R., & Stark, L. (1975). The main sequence, a tool for studying human eye movements. *Mathematical Biosciences*, *24*(3), 191-204. doi:[https://doi.org/10.1016/0025-5564\(75\)90075-9](https://doi.org/10.1016/0025-5564(75)90075-9)
- Batista, A. (2020). Chapter 17 - Brain-computer interfaces for basic neuroscience. In N. F. Ramsey & J. d. R. Millán (Eds.), *Handbook of Clinical Neurology* (Vol. 168, pp. 233-247): Elsevier.
- Becker, W., & Jürgens, R. (1979). An analysis of the saccadic system by means of double step stimuli. *Vision research*, *19*(9), 967-983.
- Blohm, G., Missal, M., & Lefèvre, P. (2003). Interaction between smooth anticipation and saccades during ocular orientation in darkness. *Journal of neurophysiology*, *89*(3), 1423-1433.
- Bourrelly, C., Quinet, J., & Goffart, L. (2015). Evolution of the oculomotor tracking with an accelerating or decelerating target. *Journal of Vision*, *15*(12), 1016-1016. doi:10.1167/15.12.1016
- Braff, D. L., & Geyer, M. A. (1990). Sensorimotor gating and schizophrenia: human and animal model studies. *Archives of general psychiatry*, *47*(2), 181-188.
- Bryant, C. L., & Gandhi, N. J. (2005). Real-time data acquisition and control system for the measurement of motor and neural data. *Journal of neuroscience methods*, *142*(2), 193-200.
- Cassanello, C. R., Nihalani, A. T., & Ferrera, V. P. (2008). Neuronal Responses to Moving Targets in Monkey Frontal Eye Fields. *Journal of neurophysiology*, *100*(3), 1544-1556. doi:10.1152/jn.01401.2007
- Chan, F., Armstrong, I. T., Pari, G., Riopelle, R. J., & Munoz, D. P. (2005). Deficits in saccadic eye-movement control in Parkinson's disease. *Neuropsychologia*, *43*(5), 784-796. doi:<https://doi.org/10.1016/j.neuropsychologia.2004.06.026>

- Chuong, A. S., Miri, M. L., Busskamp, V., Matthews, G. A. C., Acker, L. C., Sørensen, A. T., . . . Boyden, E. S. (2014). Noninvasive optical inhibition with a red-shifted microbial rhodopsin. *Nature neuroscience*, *17*(8), 1123-1129. doi:10.1038/nn.3752
- Churchland, M. M., Byron, M. Y., Ryu, S. I., Santhanam, G., & Shenoy, K. V. (2006). Neural variability in premotor cortex provides a signature of motor preparation. *Journal of Neuroscience*, *26*(14), 3697-3712.
- Crawford, T., Bennett, D., Lekwuwa, G., Shaunak, S., & Deakin, J. (2002). Cognition and the inhibitory control of saccades in schizophrenia and Parkinson's disease. *Progress in brain research*, *140*, 449-466.
- Crawford, T., Goodrich, S., Henderson, L., & Kennard, C. (1989). Predictive responses in Parkinson's disease: manual keypresses and saccadic eye movements to regular stimulus events. *Journal of Neurology, Neurosurgery & Psychiatry*, *52*(9), 1033. doi:10.1136/jnnp.52.9.1033
- Dash, S., Yan, X., Wang, H., & Crawford, John D. (2015). Continuous Updating of Visuospatial Memory in Superior Colliculus during Slow Eye Movements. *Current Biology*, *25*(3), 267-274. doi:<https://doi.org/10.1016/j.cub.2014.11.064>
- de Brouwer, S., Missal, M., Barnes, G., & Lefèvre, P. (2002). Quantitative analysis of catch-up saccades during sustained pursuit. *J Neurophysiol*, *87*(4), 1772-1780. doi:10.1152/jn.00621.2001
- de Brouwer, S., Missal, M., & Lefèvre, P. (2001). Role of retinal slip in the prediction of target motion during smooth and saccadic pursuit. *Journal of neurophysiology*, *86*(2), 550-558.
- Dean, P. (1995). Modelling the role of the cerebellar fastigial nuclei in producing accurate saccades: the importance of burst timing. *Neuroscience*, *68*(4), 1059-1077. doi:[https://doi.org/10.1016/0306-4522\(95\)00239-F](https://doi.org/10.1016/0306-4522(95)00239-F)
- Dicke, P. W., Barash, S., Ilg, U. J., & Thier, P. (2004). Single-neuron evidence for a contribution of the dorsal pontine nuclei to both types of target-directed eye movements, saccades and smooth-pursuit. *European Journal of Neuroscience*, *19*(3), 609-624. doi:<https://doi.org/10.1111/j.0953-816X.2003.03137.x>
- Drucker, C. B., Carlson, M. L., Toda, K., DeWind, N. K., & Platt, M. L. (2015). Non-invasive primate head restraint using thermoplastic masks. *Journal of neuroscience methods*, *253*, 90-100.
- Eggert, T., Guan, Y., Bayer, O., & Büttner, U. (2005). Saccades to moving targets. *Annals of the New York Academy of Sciences*, *1039*(1), 149-159.
- Everling, S., Paré, M., Dorris, M. C., & Munoz, D. P. (1998). Comparison of the discharge characteristics of brain stem omnipause neurons and superior colliculus fixation neurons in monkey: implications for control of fixation and saccade behavior. *Journal of neurophysiology*, *79*(2), 511-528.

- Fletcher, W. A., & Sharpe, J. A. (1986). Saccadic eye movement dysfunction in Alzheimer's disease. *Annals of Neurology*, 20(4), 464-471. doi:<https://doi.org/10.1002/ana.410200405>
- Fleuriet, J., Hugues, S., Perrinet, L., & Goffart, L. (2011). Saccadic foveation of a moving visual target in the rhesus monkey. *Journal of neurophysiology*, 105(2), 883-895.
- Fuchs, A. F. (1967). Saccadic and smooth pursuit eye movements in the monkey. *The Journal of Physiology*, 191(3), 609-631. doi:<https://doi.org/10.1113/jphysiol.1967.sp008271>
- Fuchs, A. F., Robinson, F. R., & Straube, A. (1993). Role of the caudal fastigial nucleus in saccade generation. I. Neuronal discharge pattern. *Journal of neurophysiology*, 70(5), 1723-1740. doi:10.1152/jn.1993.70.5.1723
- Gandhi, N. J., & Katnani, H. A. (2011). Motor functions of the superior colliculus. *Annu Rev Neurosci*, 34, 205-231. doi:10.1146/annurev-neuro-061010-113728
- Gandhi, N. J., & Keller, E. L. (1999). Comparison of saccades perturbed by stimulation of the rostral superior colliculus, the caudal superior colliculus, and the omnipause neuron region. *Journal of neurophysiology*, 82(6), 3236-3253.
- Goffart, L., Bourrelly, C., & Quinton, J.-C. (2018). Neurophysiology of visually guided eye movements: critical review and alternative viewpoint. *Journal of neurophysiology*, 120(6), 3234-3245.
- Goffart, L., Cecala, A. L., & Gandhi, N. J. (2017). The superior colliculus and the steering of saccades toward a moving visual target. *Journal of neurophysiology*, 118(5), 2890-2901.
- Goffart, L., & Pélisson, D. (1998). Orienting Gaze Shifts During Muscimol Inactivation of Caudal Fastigial Nucleus in the Cat. I. Gaze Dysmetria. *Journal of neurophysiology*, 79(4), 1942-1958. doi:10.1152/jn.1998.79.4.1942
- Goossens, H., & van Opstal, A. J. (2012). Optimal control of saccades by spatial-temporal activity patterns in the monkey superior colliculus. *PLoS Comput Biol*, 8(5), e1002508.
- Groner, R., & Groner, M. T. (1989). Attention and eye movement control: An overview. *European archives of psychiatry and neurological sciences*, 239(1), 9-16. doi:10.1007/BF01739737
- Guan, Y., Eggert, T., Bayer, O., & Büttner, U. (2005). Saccades to stationary and moving targets differ in the monkey. *Experimental brain research*, 161(2), 220-232.
- Hafed, Ziad M., & Chen, C.-Y. (2016). Sharper, Stronger, Faster Upper Visual Field Representation in Primate Superior Colliculus. *Current Biology*, 26(13), 1647-1658. doi:<https://doi.org/10.1016/j.cub.2016.04.059>
- Hall, W. C., & Moschovakis, A. K. (2003). *The superior colliculus: new approaches for studying sensorimotor integration*: CRC Press.

- Hanes, D. P., & Wurtz, R. H. (2001). Interaction of the frontal eye field and superior colliculus for saccade generation. *Journal of neurophysiology*, 85(2), 804-815.
- Harting, J. K. (1977). Descending pathways from the superior colliculus: an autoradiographic analysis in the rhesus monkey (*Macaca mulatta*). *Journal of Comparative Neurology*, 173(3), 583-612.
- Harting, J. K., Hall, W. C., Diamond, I. T., & Martin, G. F. (1973). Anterograde degeneration study of the superior colliculus in *Tupaia glis*: Evidence for a subdivision between superficial and deep layers. *Journal of Comparative Neurology*, 148(3), 361-386. doi:<https://doi.org/10.1002/cne.901480305>
- Hikosaka, O., Takikawa, Y., & Kawagoe, R. (2000). Role of the Basal Ganglia in the Control of Purposive Saccadic Eye Movements. *Physiological Reviews*, 80(3), 953-978. doi:10.1152/physrev.2000.80.3.953
- Huerta, M. F. (1984). The mammalian superior colliculus: studies of its morphology and connections. *The comparative neurology of the optic tectum*, 687-772.
- Jagadisan, U. K., & Gandhi, N. J. (2019). Population temporal structure supplements the rate code during sensorimotor transformations. *bioRxiv*, 132514. doi:10.1101/132514
- Javal, E. (1878). Essai sur la physiologie de la lecture. *Annales d'Oculistique*, 80, 97-117.
- Kasap, B., & van Opstal, A. J. (2017). A spiking neural network model of the midbrain superior colliculus that generates saccadic motor commands. *Biological Cybernetics*, 111(3), 249-268. doi:10.1007/s00422-017-0719-9
- Katnani, H. A., & Gandhi, N. J. (2012). The relative impact of microstimulation parameters on movement generation. *Journal of neurophysiology*, 108(2), 528-538.
- Keller, E., Gandhi, N., & Weir, P. (1996). Discharge of superior collicular neurons during saccades made to moving targets. *Journal of neurophysiology*, 76(5), 3573-3577.
- Keller, E., & Johnsen, S. S. (1990). Velocity prediction in corrective saccades during smooth-pursuit eye movements in monkey. *Experimental brain research*, 80(3), 525-531.
- Keller, E. L., & Heinen, S. J. (1991). Generation of smooth-pursuit eye movements: neuronal mechanisms and pathways. *Neuroscience Research*, 11(2), 79-107. doi:[https://doi.org/10.1016/0168-0102\(91\)90048-4](https://doi.org/10.1016/0168-0102(91)90048-4)
- Kennard, C., & Lueck, C. J. (1989). Oculomotor abnormalities in diseases of the basal ganglia. *Revue neurologique*, 145(8-9), 587-595. Retrieved from <http://europepmc.org/abstract/MED/2530611>
- Kim, C. E., Thaker, G. K., Ross, D. E., & Medoff, D. (1997). Accuracies of saccades to moving targets during pursuit initiation and maintenance. *Exp Brain Res*, 113(2), 371-377. doi:10.1007/bf02450336

- Krauzlis, R. J., Liston, D., & Carello, C. D. (2004). Target selection and the superior colliculus: goals, choices and hypotheses. *Vision research*, *44*(12), 1445-1451.
- Landolt, E. (1891). Nouvelles recherches sur la physiologie des mouvements des yeux. *Archives d'ophtalmologie*, *11*, 385-395.
- Lee, C., Rohrer, W. H., & Sparks, D. L. (1988). Population coding of saccadic eye movements by neurons in the superior colliculus. *Nature*, *332*(6162), 357-360.
- Leigh, R. J., & Zee, D. S. (2015). *The neurology of eye movements*: OUP USA.
- Leonardo, A., & Meister, M. (2013). Nonlinear Dynamics Support a Linear Population Code in a Retinal Target-Tracking Circuit. *The Journal of Neuroscience*, *33*(43), 16971-16982. doi:10.1523/jneurosci.2257-13.2013
- Lisberger, S. G., Morris, E. J., & Tychsen, L. (1987). Visual motion processing and sensory-motor integration for smooth pursuit eye movements. *Annu Rev Neurosci*, *10*, 97-129. doi:10.1146/annurev.ne.10.030187.000525
- Massot, C., Jagadisan, U. K., & Gandhi, N. J. (2019). Sensorimotor transformation elicits systematic patterns of activity along the dorsoventral extent of the superior colliculus in the macaque monkey. *Communications Biology*, *2*(1), 287. doi:10.1038/s42003-019-0527-y
- May, P. J. (2006). The mammalian superior colliculus: laminar structure and connections. *Progress in brain research*, *151*, 321-378.
- McHaffie, J. G., & Stein, B. E. (1982). Eye movements evoked by electrical stimulation in the superior colliculus of rats and hamsters. *Brain research*, *247*(2), 243-253. doi:[https://doi.org/10.1016/0006-8993\(82\)91249-5](https://doi.org/10.1016/0006-8993(82)91249-5)
- McPeck, R. M., & Keller, E. L. (2002). Saccade target selection in the superior colliculus during a visual search task. *Journal of neurophysiology*, *88*(4), 2019-2034.
- Meredith, M. A., & Ramoa, A. S. (1998). Intrinsic circuitry of the superior colliculus: pharmacophysiological identification of horizontally oriented inhibitory interneurons. *Journal of neurophysiology*, *79*(3), 1597-1602.
- Munoz, D. P., Armstrong, I. T., Hampton, K. A., & Moore, K. D. (2003). Altered control of visual fixation and saccadic eye movements in attention-deficit hyperactivity disorder. *Journal of neurophysiology*, *90*(1), 503-514.
- Munoz, D. P., & Istvan, P. J. (1998). Lateral inhibitory interactions in the intermediate layers of the monkey superior colliculus. *Journal of neurophysiology*, *79*(3), 1193-1209.
- Munoz, D. P., & Wurtz, R. H. (1995a). Saccade-related activity in monkey superior colliculus. I. Characteristics of burst and buildup cells. *Journal of neurophysiology*, *73*(6), 2313-2333.

- Munoz, D. P., & Wurtz, R. H. (1995b). Saccade-related activity in monkey superior colliculus. II. Spread of activity during saccades. *Journal of neurophysiology*, *73*(6), 2334-2348.
- Mustari, M. J., Fuchs, A. F., & Wallman, J. (1988). Response properties of dorsolateral pontine units during smooth pursuit in the rhesus macaque. *Journal of neurophysiology*, *60*(2), 664-686.
- Nakamura, K., & Colby, C. L. (2002). Updating of the visual representation in monkey striate and extrastriate cortex during saccades. *Proceedings of the National Academy of Sciences*, *99*(6), 4026-4031. doi:10.1073/pnas.052379899
- Newsome, W. T., Wurtz, R. H., Dürsteler, M. R., & Mikami, A. (1985). Deficits in visual motion processing following ibotenic acid lesions of the middle temporal visual area of the macaque monkey. *J Neurosci*, *5*(3), 825-840. doi:10.1523/jneurosci.05-03-00825.1985
- Optican, L. M., & Quaia, C. (2002). Distributed model of collicular and cerebellar function during saccades. *Annals of the New York Academy of Sciences*, *956*(1), 164-177.
- Ottes, F. P., Van Gisbergen, J. A., & Eggermont, J. J. (1986). Visuomotor fields of the superior colliculus: a quantitative model. *Vision research*, *26*(6), 857-873.
- Péllisson, D., Goffart, L., Guillaume, A., Catz, N., & Raboyeau, G. (2001). Early head movements elicited by visual stimuli or collicular electrical stimulation in the cat. *Vision research*, *41*(25), 3283-3294. doi:[https://doi.org/10.1016/S0042-6989\(01\)00224-3](https://doi.org/10.1016/S0042-6989(01)00224-3)
- Pettit, D. L., Helms, M. C., Lee, P., Augustine, G. J., & Hall, W. C. (1999). Local Excitatory Circuits in the Intermediate Gray Layer of the Superior Colliculus. *Journal of neurophysiology*, *81*(3), 1424-1427. doi:10.1152/jn.1999.81.3.1424
- Phongphanphane, P., Marino, R. A., Kaneda, K., Yanagawa, Y., Munoz, D. P., & Isa, T. (2014). Distinct local circuit properties of the superficial and intermediate layers of the rodent superior colliculus. *European Journal of Neuroscience*, *40*(2), 2329-2343.
- Phongphanphane, P., Mizuno, F., Lee, P. H., Yanagawa, Y., Isa, T., & Hall, W. C. (2011). A Circuit Model for Saccadic Suppression in the Superior Colliculus. *The Journal of Neuroscience*, *31*(6), 1949-1954. doi:10.1523/jneurosci.2305-10.2011
- Quinet, J., & Goffart, L. (2015). Does the brain extrapolate the position of a transient moving target? *Journal of Neuroscience*, *35*(34), 11780-11790.
- Raiguel, S., Van Hulle, M., Xiao, D. K., Marcar, V., & Orban, G. A. (1995). Shape and spatial distribution of receptive fields and antagonistic motion surrounds in the middle temporal area (V5) of the macaque. *European Journal of Neuroscience*, *7*(10), 2064-2082.
- Rashbass, C. (1961). The relationship between saccadic and smooth tracking eye movements. *The Journal of Physiology*, *159*(2), 326-338. doi:10.1113/jphysiol.1961.sp006811

- Reuter, B., & Kathmann, N. (2004). Using saccade tasks as a tool to analyze executive dysfunctions in schizophrenia. *Acta psychologica, 115*(2-3), 255-269.
- Richmond, B. J., Optican, L. M., Podell, M., & Spitzer, H. (1987). Temporal encoding of two-dimensional patterns by single units in primate inferior temporal cortex. I. Response characteristics. *Journal of neurophysiology, 57*(1), 132-146. doi:10.1152/jn.1987.57.1.132
- Robinson, D. A. (1972). Eye movements evoked by collicular stimulation in the alert monkey. *Vision research, 12*(11), 1795-1808.
- Robinson, D. A. (1973). Models of the saccadic eye movement control system. *Kybernetik, 14*(2), 71-83.
- Ron, S., Vieville, T., & Droulez, J. (1989). Target velocity based prediction in saccadic vector programming. *Vision Res, 29*(9), 1103-1114. doi:10.1016/0042-6989(89)90059-x
- Schlag, J., & Schlag-Rey, M. (2002). Through the eye, slowly; Delays and localization errors in the visual system. *Nature Reviews Neuroscience, 3*(3), 191-191.
- Scudder, C. A. (2002). Role of the Fastigial Nucleus in Controlling Horizontal Saccades during Adaptation. *Annals of the New York Academy of Sciences, 978*(1), 63-78. doi:<https://doi.org/10.1111/j.1749-6632.2002.tb07556.x>
- Segraves, M. A. (1992). Activity of monkey frontal eye field neurons projecting to oculomotor regions of the pons. *Journal of neurophysiology, 68*(6), 1967-1985.
- Smalianchuk, I., Jagadisan, U. K., & Gandhi, N. J. (2018). Instantaneous midbrain control of saccade velocity. *Journal of Neuroscience, 38*(47), 10156-10167.
- Sparks, D. L., & Hartwich-Young, R. (1989). The deep layers of the superior colliculus. *Rev Oculomot Res, 3*, 213-255.
- Sparks, D. L., & Hu, X. (2006). *Saccade initiation and the reliability of motor signals involved in the generation of saccadic eye movements*. Paper presented at the Novartis Foundation Symposium.
- Stanford, T. R., Freedman, E. G., & Sparks, D. L. (1996). Site and parameters of microstimulation: evidence for independent effects on the properties of saccades evoked from the primate superior colliculus. *Journal of neurophysiology, 76*(5), 3360-3381. doi:10.1152/jn.1996.76.5.3360
- Straschill, M., & Rieger, P. (1973). Eye movements evoked by focal stimulation of the cats superior colliculus. *Brain research, 59*, 211-227. doi:[https://doi.org/10.1016/0006-8993\(73\)90262-X](https://doi.org/10.1016/0006-8993(73)90262-X)
- Straube, A., Fuchs, A. F., Usher, S., & Robinson, F. R. (1997). Characteristics of Saccadic Gain Adaptation in Rhesus Macaques. *Journal of neurophysiology, 77*(2), 874-895. doi:10.1152/jn.1997.77.2.874

- T Raphan, a., & Cohen, B. (1978). Brainstem Mechanisms for Rapid and Slow Eye Movements. *Annual Review of Physiology*, 40(1), 527-552. doi:10.1146/annurev.ph.40.030178.002523
- Terao, Y., Fukuda, H., Yugeta, A., Hikosaka, O., Nomura, Y., Segawa, M., . . . Ugawa, Y. (2011). Initiation and inhibitory control of saccades with the progression of Parkinson's disease—changes in three major drives converging on the superior colliculus. *Neuropsychologia*, 49(7), 1794-1806.
- Thier, P., Koehler, W., & Buettner, U. (1988). Neuronal activity in the dorsolateral pontine nucleus of the alert monkey modulated by visual stimuli and eye movements. *Experimental brain research*, 70(3), 496-512.
- Ungerleider, L. G., Desimone, R., Galkin, T. W., & Mishkin, M. (1984). Subcortical projections of area MT in the macaque. *Journal of Comparative Neurology*, 223(3), 368-386.
- Wall, J. T., Symonds, L. L., & Kaas, J. H. (1982). Cortical and subcortical projections of the middle temporal area (MT) and adjacent cortex in galagos. *Journal of Comparative Neurology*, 211(2), 193-214. doi:<https://doi.org/10.1002/cne.902110208>
- Westheimer, G. (1954). Mechanism of saccadic eye movements. *AMA archives of ophthalmology*, 52(5), 710-724.
- White, O. B., Saint-Cyr, J. A., Tomlinson, R. D., & Sharpe, J. A. (1983). Ocular Motor Deficits in Parkinson's Disease: II. Control of the Saccadic and Smooth Pursuit Systems. *Brain*, 106(3), 571-587. doi:10.1093/brain/106.3.571
- Wurtz, R. H., & Goldberg, M. E. (1972). Activity of superior colliculus in behaving monkey. 3. Cells discharging before eye movements. *Journal of neurophysiology*, 35(4), 575-586. doi:10.1152/jn.1972.35.4.575
- Wurtz, R. H., Sommer, M. A., Paré, M., & Ferraina, S. (2001). Signal transformations from cerebral cortex to superior colliculus for the generation of saccades. *Vision research*, 41(25), 3399-3412. doi:[https://doi.org/10.1016/S0042-6989\(01\)00066-9](https://doi.org/10.1016/S0042-6989(01)00066-9)